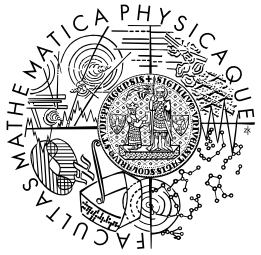

FACULTY
OF MATHEMATICS
AND PHYSICS
Charles University

MASTER THESIS

Petr Lukeš

Emergence of space geometries from quantum entanglement

Institute of Theoretical Physics

Supervisor of the master thesis:	Mgr. Martin Scholtz, Ph.D.
Study programme:	Physics
Study branch:	Theoretical physics

Prague 2019

I declare that I carried out this master thesis independently, and only with the cited sources, literature and other professional sources.

I understand that my work relates to the rights and obligations under the Act No. 121/2000 Sb., the Copyright Act, as amended, in particular the fact that the Charles University has the right to conclude a license agreement on the use of this work as a school work pursuant to Section 60 subsection 1 of the Copyright Act.

In ..... date ..... signature of the author

I would like to dedicate this work to my mother Blanka, father Zdeněk and brother Zdeněk. It was only their endless support throughout all my studies which helped me continue even when I would not have enough strength on my own.

Thank you

Title: Emergence of space geometries from quantum entanglement

Author: Petr Lukeš

Institute: Institute of Theoretical Physics

Supervisor: Mgr. Martin Scholtz, Ph.D., Institute of Theoretical Physics

Abstract: Connecting the field of Quantum Physics and General Relativity is one of the main interests of contemporary Theoretical Physics. This work attempts to find solution to simplified version of this problem. Firstly entropy is shown to be a good meeting point between the two different theories. Then some of entropy's less intuitive properties are shown, namely its dependence on area, not volume. This relation is studied from both Relativistic and Quantum viewpoint. Afterwards there is a short description of a quantum model interpretable as geometry based on the information between its subsystems. Lastly, results of computations within this model are presented.

Keywords: Emergent geometry, Redundancy Constraint, Bekenstein limit, Hawking radiation

Contents

Introduction

Our world is to the best of our knowledge governed by four fundamental interactions. Electromagnetic, weak, strong and gravitational. With the usage of Quantum Field Theory a unified description of the first three can be derived, this being known as Standard Model and its extensions. On the other hand the last interaction, gravitational, remains from this point of view elusive.

In the last decades many models of inclusion of gravitation to the Standard Model have been proposed but none was found completely satisfactory. And so the task of unifying gravitation with the rest of the fundamental interactions remains among the most interesting and important problems of contemporary theoretical physics.

As mentioned, our current understanding of the three unified interactions is based on their quantum description. So it is natural to search for such description of the gravitation too, as only when that is found we can put all fundamental interactions onto common grounds. And such complete theory, known as Theory of Everything, is one of the ultimate goals of the current theoretical physics.

But let us get back down to earth. The initial problem still being solved these days is how to describe gravitation on the quantum level. Some at least partial models have been already proposed, for example in the field of string physics, or for QFT on curved background. From other considerations we even know what we should expect from the resulting theory of quantum gravity (e.g. we know that the particle mediating the gravitation interaction, which we call graviton, has to have spin 2). As far as this work is concerned it is the AdS/CFT correspondence [1] which sparked the considerations included in this work (admittedly without exact understanding of the AdS/CFT itself).

In this work the entropy is chosen to be the meeting point between geometry and quantum theory. On the gravitation side the entropy of a black hole is well known from basic consideration of black hole thermodynamics and is found to be proportional only to the surface area of the black hole's event horizon

$$S = \frac{1}{4}\frac{A}{G_N}. \tag{1}$$

In this equation S is the entropy, A area and G_N Newton's constant, $\hbar$ and c are both assumed to be equal to 1. On the other hand in quantum information theory the entropy is defined via the eigenvalues of the density matrix $\hat{\rho}$ (and such matrix can be ascribed to each quantum state)

$$S = -\sum_{p_j \in \sigma(\hat{\rho})} p_j \ln(p_j) \tag{2}$$

$$\hat{\rho}\,|\phi_j\rangle = p_j\,|\phi_j\rangle\,. \tag{3}$$

So the aim is to find such quantum state living on some Hilbert space of known structure, that the subspaces of the Hilbert space can be interpreted as points of some metric space. The distance between those points is computed from the entanglement entropy. Several methods of embedding the points into metric space are investigated in this work. In general the metric space with the set of embedded points is called the emergent geometry.

Because the field of emergent geometry is a contemporary problem and there is not yet much of an established formalism, this work focuses mainly on trial and error approach for finding some quantum states capable of representing a geometry via computational methods. It will be shown that such states are quite rare and so are even the Hilbert spaces capable of representing them.

The structure of this work is as follows: The first chapter contains a glimpse at some theoretical findings connected to the topic of this work. This part is the largest in this work yet is anything but exhaustive. In the second chapter the computational methods employed in this work are commented upon. In the third chapter the results of the computation are shown with some commentary and comparison to the results of other works in the end.

1. Preliminaries

1.1 Properties of entropy

Entropy is a concept firstly introduced for quantitative description of irreversible processes in the field of thermodynamics. Its statistical interpretation is that it describes the lack of information. The higher the entropy, the more generic and without precise information is the available description of the system. It is an observed fact that during all ongoing processes in the nature, the total entropy of the Universe always increases (known as 2nd Law of Thermodynamics).

Entropy can be also attributed to quantum states. Assume a mixed quantum state $\{p_i, |\psi_i\rangle\}_{i=1}^{N}$, where N is the number of the states and p_j is the probability to find the system in the state $|\psi_j\rangle$. Then we can ascribe to this mixed state corresponding density operator (in the field of statistical physics also known as statistical operator) by relation

$$\hat{\rho} = \sum_{i=1}^{N} q_i \, |\psi_i\rangle\langle\psi_i| \, . \tag{1.1}$$

The spectrum of this density operator is $\sigma(\hat{\rho}) = \{p_1, \ldots, p_n\}$ and the entropy S is defined as

$$S = -\operatorname{Tr}(\hat{\rho}\ln(\hat{\rho})) = -\sum_{p_j \in \sigma(\hat{\rho})} p_j \ln(p_j). \tag{1.2}$$

The entropy defined by (1.2) is called Von Neumann entropy (as opposed to entropy in thermodynamics and Gibbs/Shannon entropy in statistical physics and information theory[1]). When entropy is mentioned in the following text, it is understood to be the Von Neumann entropy. Some of its interesting properties are the following.

Firstly, entropy is always greater than or equal to zero. This can be seen from Figure 1.1, as the values p_j from the definition (1.2) is a probability and so needs to be always between 0 and 1. Also, for pure states, it is always 0 as then the corresponding density matrix is a projector onto the space of the pure state $\hat{\rho} = |\psi\rangle\langle\psi|$. The reason is that then $\hat{\rho}$ has only two eigenvalues $\{+1,0\}$ and, looking at the Figure 1.1, it is obvious, that it is zero at 1 and its limit from the right is zero at 0 too. This is in agreement with the meaning of entropy as a measure of ignorance, as at pure state, we know precisely the exact state of the system. On the contrary, entropy is obviously not equal to zero for general mixed states since it is nonzero for all values of p_j between 0 and 1.

Secondly, entropy can be also shown to have its maximum at uniform distribution. Assume a maximally nondiscriminating state $|\Psi_{MND}\rangle$ on the Hilbert space $\mathscr{H}$ of dimension D, which is a mixed state $|\Psi_{MND}\rangle = \{\frac{1}{D}, |\psi_i\rangle\}_{i=1}^{D}$ and $\langle\psi_i|\psi_j\rangle = \delta_{ij}$, so the set $\{|\psi_i\rangle\}_{i=1}^{D}$ is an orthonormal basis in $\mathscr{H}$. Then the

[1] While each of the type of entropy can be traced to correspond to every other, they are differed one from another as they are results of different approaches towards the problem of statistical description

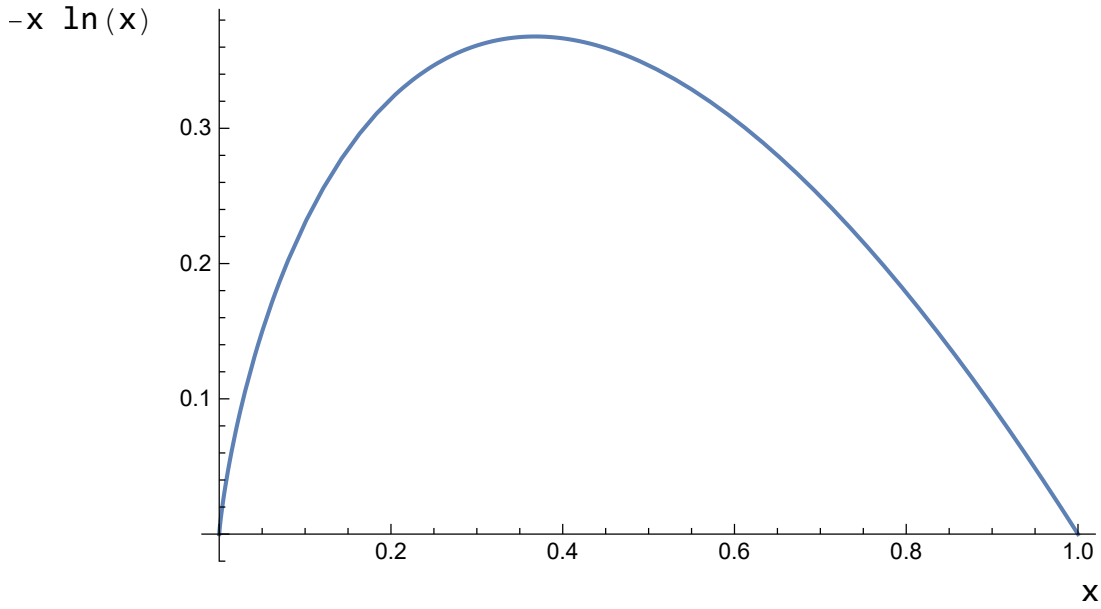

Figure 1.1: Plot of the function $-x\ln(x)$ corresponding to the definition of the entropy

entropy corresponding to this state is

$$S = -\sum_{p_j \in \sigma(\hat{\rho}_{MND})} \frac{1}{D}\ln\left(\frac{1}{D}\right) = \ln(D). \tag{1.3}$$

Now assume the so-called relative statistical entropy [2]

$$S(\hat{\rho}|\hat{\rho}_0) = \mathrm{Tr}(\hat{\rho}\ln(\hat{\rho}) - \hat{\rho}\ln(\hat{\rho}_0)). \tag{1.4}$$

Assuming $\hat{\rho}$ and $\hat{\rho}_0$ can be expressed in the orthonormal eigenbasis $|\phi_i\rangle$ as $\hat{\rho} = \sum_{\sigma(\hat{\rho})} p_j \,|\phi_j\rangle\langle\phi_j|$ and $\hat{\rho}_0 = \sum_{\sigma(\hat{\rho}_0)} q_j \,|\phi_j\rangle\langle\phi_j|$ it follows that

$$S(\hat{\rho}|\hat{\rho}_0) = \sum_j p_j\ln(p_j) - p_j\ln(q_j) \tag{1.5}$$

It can be seen that if

$$\hat{\rho}_0 = \hat{\rho}_{MND} = \frac{1}{D}\sum_{j=1}^{D} |\psi_j\rangle\langle\psi_j| = \frac{1}{D}\hat{\mathbb{1}}, \tag{1.6}$$

then $\hat{\rho}_{MND}$ has the same form with respect to any basis. So

$$S(\hat{\rho}|\hat{\rho}_{MND}) = \sum_{j=1}^{D} p_j\ln(p_j) - p_j\ln\left(\frac{1}{D}\right) = \ln(D) + \sum_{j=1}^{D} p_j\ln(p_j) = \ln(D) - S(\hat{\rho}) \tag{1.7}$$

exploiting $\sum\limits_{j=1}^{D} p_j = 1$ as p_j is a probability.

It can be also shown, that $\forall\hat{\rho},\hat{\rho}_0 : S(\hat{\rho}|\hat{\rho}_0) \geq 0$. For the special case of $\hat{\rho}_0 = \hat{\rho}_{MND} = \frac{1}{D}\hat{\mathbb{1}}$ the proof is easy, as then $\forall x \in (0,1) : \ln(1+x) \leq x$ and so

$$\begin{aligned} S(\hat{\rho}|\hat{\rho}_{MND}) &= \sum_{j=1}^{D} p_j\ln(p_j) - p_j\ln\left(\frac{1}{D}\right) = -\sum_{j=1}^{D} p_j\ln\left(\frac{1}{Dp_j}\right) \geq \\ &\geq -\sum_{j=1}^{D} p_j\left(\frac{1}{Dp_j} - 1\right) = \sum_{j=1}^{D} p_j - 1/D = 1 - 1 = 0. \end{aligned} \tag{1.8}$$

As a result, $S(\hat{\rho}|\hat{\rho}_{MND}) = \ln(D) - S(\hat{\rho}) \geq 0$, so $S(\hat{\rho}) \leq \ln(D)$ and it has been shown above, that $\hat{\rho} = \hat{\rho}_{MND} \implies S(\hat{\rho}) = \ln(D)$. The implication can be proven also in the opposite direction (uniqueness of the maximum of the entropy), but this is not a part of this work.

Thirdly, entropy can be shown to be concave. This means that if 2 density operators $\hat{\rho}_1$ and $\hat{\rho}_2$ and a real number λ are found so that $\hat{\rho} = \lambda\hat{\rho}_1 + (1-\lambda)\hat{\rho}_2$ than $S(\hat{\rho}) \geq \lambda S(\hat{\rho}_1) + (1-\lambda)S(\hat{\rho}_2)$.

Lemma 1. *Klein's inequality. Let $\hat{A}$ and $\hat{B}$ be self-adjoint operators and $f : \mathbb{R} \to \mathbb{R}$ be a convex function. Then*

$$\mathrm{Tr}(f(A) - f(B) - (A-B)f'(B)) \geq 0.$$

Proof: Assume two orthonormal bases $\{|a_i\rangle\}_{i=1}^{D}$ and $\{|b_i\rangle\}_{i=1}^{D}$ such, that $\hat{A}\,|a_i\rangle = a_i\,|a_i\rangle$ and $\hat{B}\,|b_i\rangle = b_i\,|b_i\rangle$. Then

$$\mathrm{Tr}\Big(f(\hat{A}) - f(\hat{B}) - (\hat{A}-\hat{B})f'(\hat{B})\Big) = \sum_{i=1}^{D} \langle a_i|\, f(\hat{A}) - f(\hat{B}) - (\hat{A}-\hat{B})f'(\hat{B})\,|a_i\rangle =$$

$$= \sum_{i=1}^{D} f(a_i) - \langle a_i|\, f(\hat{B})\,|a_i\rangle - a_i\,\langle a_i|\, f'(\hat{B})\,|a_i\rangle + \langle a_i|\,\hat{B}f(\hat{B})\,|a_i\rangle = \dots$$

Adding unity in the form $\hat{\mathbb{1}} = \sum_{i=1}^{N} |b_j\rangle\langle b_j|$ next to each operator $\hat{B}$ or its function then leads to

$$\cdots = \sum_{i,j=1}^{N} |\langle a_i|b_j\rangle|^2 (f(a_i) - f(b_j) - (a_i - b_j)f'(b_j)).$$

And since one of the definitions of convexity of f is $\forall x,y \in \mathscr{D}(f) : f(x) \geq f(y) + (x-y)f'(y)$ ($\mathscr{D}(f)$ is the domain of the function f) and since $|\langle a_i|b_j\rangle|^2 \geq 0$ always, the Klein's inequality is proven. □

Now assume $f(x) = x\ln(x)$ which is a convex function on the interval $(0, +\infty)$ and so the Klein's inequality gives:

$$\begin{aligned} &\mathrm{Tr}\Big(\hat{A}\ln\Big(\hat{A}\Big) - \hat{B}\ln\Big(\hat{B}\Big) - (\hat{A}-\hat{B})(1+\ln\Big(\hat{B}\Big))\Big) = \\ &\qquad = \mathrm{Tr}\Big(\hat{A}\ln\Big(\hat{A}\Big) - \hat{A}\ln\Big(\hat{B}\Big) - (\hat{A}-\hat{B})\Big) \geq 0 \end{aligned} \tag{1.9}$$

Now there are two cases in which (1.9) will be applied.

$$\begin{aligned} &\hat{A} = \hat{\rho}_1,\ \hat{B} = \lambda\hat{\rho}_1 + (1-\lambda)\hat{\rho}_2 \\ \implies &\mathrm{Tr}(\hat{\rho}_1\ln(\hat{\rho}_1) - \hat{\rho}_1\ln(\lambda\hat{\rho}_1 + (1-\lambda)\hat{\rho}_2) - (\hat{\rho}_1 - \lambda\hat{\rho}_1 - (1-\lambda)\hat{\rho}_2)) = \dots \\ &\mathrm{Tr}(\hat{\rho}_1) = 1, \mathrm{Tr}(\hat{\rho}_2) = 1 \\ \cdots = &\mathrm{Tr}(\hat{\rho}_1\ln(\hat{\rho}_1) - \hat{\rho}_1\ln(\lambda\hat{\rho}_1 + (1-\lambda)\hat{\rho}_2))) \geq 0 \end{aligned} \tag{1.10}$$

$$\begin{aligned} &\hat{A} = \hat{\rho}_2,\ \hat{B} = \lambda\hat{\rho}_1 + (1-\lambda)\hat{\rho}_2 \\ \implies &\mathrm{Tr}(\hat{\rho}_2\ln(\hat{\rho}_2) - \hat{\rho}_2\ln(\lambda\hat{\rho}_1 + (1-\lambda)\hat{\rho}_2) - (\hat{\rho}_2 - \lambda\hat{\rho}_1 - (1-\lambda)\hat{\rho}_2)) = \\ = &\mathrm{Tr}(\hat{\rho}_2\ln(\hat{\rho}_2) - \hat{\rho}_2\ln(\lambda\hat{\rho}_1 + (1-\lambda)\hat{\rho}_2))) \geq 0 \end{aligned} \tag{1.11}$$

Multiplying (1.10) by λ and (1.11) by $(1-\lambda)$ and adding those gives

$$\begin{aligned}&\mathrm{Tr}(\lambda\hat{\rho}_1\ln(\hat{\rho}_1)-\lambda\hat{\rho}_1\ln(\lambda\hat{\rho}_1+(1-\lambda)\hat{\rho}_2)+(1-\lambda)\hat{\rho}_2\ln(\hat{\rho}_2)-(1-\lambda)\hat{\rho}_2\ln(\lambda\hat{\rho}_1+(1-\lambda)\hat{\rho}_2)))=\\&=\mathrm{Tr}(\lambda\hat{\rho}_1\ln(\hat{\rho}_1)+(1-\lambda)\hat{\rho}_2\ln(\hat{\rho}_2)-(\lambda\hat{\rho}_1+(1-\lambda)\hat{\rho}_2)\ln(\lambda\hat{\rho}_1+(1-\lambda)\hat{\rho}_2))\geq 0\implies\end{aligned}$$

$$\implies \mathrm{Tr}(\lambda\hat{\rho}_1\ln(\hat{\rho}_1)+(1-\lambda)\hat{\rho}_2\ln(\hat{\rho}_2))\geq \mathrm{Tr}((\lambda\hat{\rho}_1+(1-\lambda)\hat{\rho}_2)\ln(\lambda\hat{\rho}_1+(1-\lambda)\hat{\rho}_2))\iff$$

$$\iff \lambda S(\hat{\rho}_1)+(1-\lambda)S(\hat{\rho}_2)\leq S(\lambda\hat{\rho}_1+(1-\lambda)\hat{\rho}_2)=S(\hat{\rho}) \qquad (1.12)$$

recalling the minus sign in (1.2). This proves the concavity of entropy.

Although the increase of entropy is considered as a well-established fact, at deeper level it seems quite mysterious. In classical physics, the rules of statistical mechanics are derived from Hamilton equations that are reversible in time. They also imply the Liouville theorem which asserts that any initial uncertainty of the state remains constant in time. In other words, phase volume is constant during Hamiltonian evolution hence the entropy should remain constant as well during the evolution. The same argument applies in quantum mechanics where the evolution of the wave function is given by a unitary, therefore invertible, operator. This fact is often referred to as the principle of conservation of information and is an important consideration for example for the black hole information paradox.

There are two explanations why the entropy increases in the real world. The first one is related to the process of coarse graining of the phase space. Since the precision of any measurement is not infinite, close points in the phase space are indistinguishable. Therefore, one has to divide the phase space into cells of finite size. As the system with many degrees of freedom evolves, the initial phase volume is conserved from a microscopic point of view, but it acquires complicated shape, often with fractal structure. Consequently, the phase volume "hits" more and more indistinguishable cells and, thus, from a macroscopic point of view, the entropy increases [3].

Another argument addresses the probability of states: system is supposed to evolve to the most probable state which is an equilibrium state. However, by reversibility, it is more probable that the entropy will increase in time, but also that the entropy was higher in the past. In other words, it is more likely that a lower (less probable) entropy state is a result of a fluctuation from (more probable) equilibrium than that evolved from even more improbable state with even smaller entropy. Hence, since we observe a systematic increase of entropy, it must be the case that the initial conditions for our universe had to be very special, with very low entropy. This rises another question. From the cosmic microwave background (CMB) we know that matter close to Big Bang was in thermal equilibrium, because CMB exhibits Planck distribution with astonishing accuracy. Thermal equilibrium is usually considered as the highest entropy state. Still, since then the entropy just increases. It seems plausible that usual thermodynamic picture must be modified when gravity becomes relevant. Similar considerations have led to many interesting ideas, e.g. Weyl curvature hypothesis and Conformal cyclic cosmology [4].

1.2 Area law of entropy

This short summary is mainly rephrasing the initial part of [5].

In this work the assumption is many times used that the entropy corresponding to a part of space whose interior cannot be accessed is proportional to the area of the surface of this region. Even though such result is acquired in Theory of Relativity for black holes (where the entropy is $S_{BH} = \frac{1}{4}M_{Pl}^2 A$, M_{Pl} denoting Planck mass and A the area of the event horizon, it is equivalent to (2) recalling that convention there is $\hbar = 1$ and c $= 1$ while it also holds that $M_{Pl} = \sqrt{\frac{\hbar c}{G_N}}$), it can be viewed as counter-intuitive from the standpoint of, for example, classical thermodynamics. There the entropy is an extensive quantity and assuming a sphere with radius R, one could expect its entropy to grow as R^3. But now a few basic arguments of the article [5] need to be considered.

Assume a simple scalar quantum field, a massless one, being in its ground state. Assume a region of the shape of a sphere which is inaccessible and so when computing the entropy of the quantum state the density matrix corresponding to the state must be traced over the degrees of freedom inside the sphere. This can be schematically represented as follows:

Let

$$|0\rangle = \sum_{io} \psi_{io} \, |i\rangle|o\rangle \tag{1.13}$$

$$\hat{D} = |0\rangle\langle 0| \tag{1.14}$$

where $|0\rangle$ is the vacuum state of the field and is divided into a direct product of the field inside (indexed with i) and outside (index o) of a sphere. As the inner degrees of freedom are inaccessible, we trace over them, e.g.

$$\hat{D}_o = \mathrm{Tr}_i(\hat{D}) = \sum_{o_1, o_2, i} \psi_{o_1 i} \psi^*_{o_2 i} \, |o_1\rangle\langle o_2| \tag{1.15}$$

and so the elements of the density matrix are $D_{o\ o_1 o_2} = (\psi\psi^\dagger)_{o_1 o_2}$.

On the other hand, imagining the inverse problem, where only the inner degrees of freedom are accessible, the density matrix traced over the outer part will be

$$\hat{D}_i = \mathrm{Tr}_o(\hat{D}) = \sum_{i_1, i_2, o} \psi_{o i_1} \psi^*_{o i_2} \, |i_1\rangle\langle i_2| \tag{1.16}$$

and the elements of the density matrix will be $D_{i\ i_1 i_2} = (\psi^T \psi^*)_{i_1 i_2}$.

Obviously, $\mathrm{Tr}_i(D_i) = \mathrm{Tr}_o(D_o)$ as both are equal to the complete trace $\mathrm{Tr}(D)$. Moreover, because $\mathrm{Tr}(A) = \mathrm{Tr}\left(A^T\right)$, it also holds $\mathrm{Tr}_i((\psi^T\psi^*)^k) = \mathrm{Tr}_o((\psi\psi^\dagger)^k)$ for any k integer and this in turn implies that D_i and D_o have the same eigenvalues up to zeros for the larger matrix. So both density operators give the same entropy (defined as 1.2).

As a result the entropy of a system where we ignore some spherical region is the same as the entropy of the system where only that spherical region is accessible. So it is natural to attribute the entropy to a common feature of both of those cases, which is the surface of the sphere (obviously the exact shape of the region is not deciding to the considerations of this section).

1.3 Redundancy constrained states

As stated in the Introduction the entropy of a region in space should be proportional to its surface area (see equation (1)). A small generalization to this principle can be done in line with [6], section II. B and III. A. Firstly let us define *area-law states* as states representing a geometry in which the entropy of an region can be determined by formula

$$S = \eta A + \dots \tag{1.17}$$

where η represents a constant of proportionality and the $\dots$ refers to additional sub-dominant terms. Above some scale the entanglement structure of area-law state captures the structure of the Hilbert space on which the area-law state is defined and where we assume some preferred decomposition into subspaces. By *entanglement structure* we mean the quantum entropy determined for each subsystem from the density matrix of the whole system traced over the subspace corresponding to the given subsystem

$$S_B = -\operatorname{Tr}(\hat{\rho}_B \ln(\hat{\rho}_B)), \tag{1.18}$$

$$\hat{\rho}_B = \operatorname{Tr}_B(\hat{\rho}) \tag{1.19}$$

and we ascribe the resulting value to the subsystem as its *entanglement entropy*.

The entanglement structure of area-law states is remarkable because it can be well approximated by mutual information between certain subsystems, instead of the defining relation (1.18). Mutual information between disjoint regions B, C is defined as

$$I(B,C) = S(B) + S(C) - S(B,C), \tag{1.20}$$

where $S(B) = -\operatorname{Tr}\left(\hat{\rho}_{\mathcal{C}(B)} \ln\left(\hat{\rho}_{\mathcal{C}(B)}\right)\right)$ (this can be viewed as definition, but according to Section 1.2 it is the same as (1.18)), $S(B,C) = S(B \cup C)$, B is a subsystem of the total system and $\mathcal{C}(B)$ is its complement, also keep in mind (1.19).

Partitioning the total system into set of subsystems $\{B_p\}$ and computing the mutual information between each pair of subsystems $I(B_j,B_k)$ the claim is that for $X \subset \{B_p\}$ the entanglement entropy can be approximated[6] as

$$S(X) = \frac{1}{2} \sum_{p \in X,\ q \in \mathcal{C}(X)} I(B_p,B_q). \tag{1.21}$$

This situation can be imagined as a graph of vertices connected by edges where each vertex corresponds to one of the subsystems B_p and each edge is weighted by the mutual information between the two connected subsystems. Then $\{B_p\}$ is the set of vertices and the entanglement entropy of its subset X is given by the total of the weights of all edges connecting the vertices of X with the vertices outside of X.

This procedure can be followed from the opposite direction resulting in a slight generalization of area-law states. Let us consider a system consisting of subsystems such, that its total Hilbert space $\mathscr{H}$ is a direct product of Hilbert spaces corresponding to those subsystems $\mathscr{H} = \bigotimes_p \mathscr{H}_p$. If, for given state, the entanglement entropy for any subset of the spaces $X \subset \{\mathscr{H}_p\}$ is given by the equation (1.21), then we call the state *redundancy constrained*.

The simplistic structure of entanglement entropy in this case allows attempts for numerical solutions to the problem of finding a state interpretable as geometry and some field theory on that geometry. The idea is that for the case where we can compute the full entanglement entropy (1.18) and also its redundancy constrained version (1.21) it is also possible to asses, if the given state is redundancy constrained. And according to [6] such states are the ones to be interpreted as a space with geometric and field content.

1.4 Lattice structure

As was proposed in Section 1.2, it is reasonable to expect the entropy of a local region (e.g. occupied by a black hole) to be proportional to its surface area. If there were degrees of freedom not contributing to the total entropy, one could excite those and either increase the entropy via entanglement of these degrees of freedom with the outer ones (outside the region) or the black hole would expand out of the borders. Thus it is reasonable to expect all available degrees of freedom to contribute to entropy. And, as finite entropy corresponds to a quantum state on finite-dimensional Hilbert space (or at least finite number of states above the vacuum, see (1.44) and considerations there), we can expect the Hilbert space of any geometric region to be finite-dimensional. This line of reasoning is more developed in [7].

Assuming we have more than one such region, the complete Hilbert space is a tensor product of individual Hilbert spaces of the regions. One might than want to imagine a geometry at least approximately as a lattice of such regions where we have some sense of distance between each pair of those. It is quite obvious that the number of such regions will be considerably high and so will be the dimension of the total Hilbert space.

Now assume that we are given a theory with general Hilbert space of some dimension n. How probable it is that it will be a space of a lattice of finite dimensional subspaces? Consider such large Hilbert space's dimension. It needs to be a product of many integers as all subspaces have integer dimension. Each dimension of a subspace is product of some primes and so is in effect the total space's dimension. Now let us see how many primes do general integers have. It has been proven by Hardy and Ramanujan [8] that for large integers N, the number of primes which N is a product of, called $\Omega(N)$[2], can be estimated as

$$\Omega(N) = \ln(\ln(N)) \tag{1.22}$$

This is a very slowly growing function and so, to attain a number with large number of primes one needs to look among extremely high integers. As a result, if one looks for a Hilbert space corresponding to a tensor product of large number of subspaces, he generally needs to search among extremely high-dimensional spaces, as only those tend to have enough of different primes to correspond to the dimensions of the smaller subspaces. From different perspective: the ratio of Hilbert spaces which can represent a lattice of high number of subspaces versus

[2] $\Omega(N)$ is defined to count repeating primes in the factorization of N separately. Function $\omega(N)$ is defined to count only unique primes, it can be shown that for large N these two functions behave equally.

all Hilbert spaces goes quickly to very low values. Thus assuming that Hilbert spaces of all dimensions are equally probable to occur, those which can represent a lattice of subspaces are the more rare, the higher their dimension. There is slightly more discussion of this point in [9].

1.5 Entropy and information on black holes

One of the strong arguments supporting the idea that gravity is in fact an emergent phenomenon is related to the black hole information paradox. Although initially there has been some controversy about the real existence of black holes [10], theorems of Penrose [11] have shown that the formation of singularity during gravitational collapse is inevitable provided that the mass of the object is sufficient. Later, the so-called no-hair theorem has been established [12, 13, 14] which states that after the collapse, black hole is fully characterized by just a few parameters, namely its mass, angular momentum and electric or magnetic charge. In fact, there are exceptions, for example gravity coupled to complex scalar fields may lead to the creation of the scalar hair [15], but the principle remains unaltered: details about collapsing matter dissapear and the only remaining information can be encoded in a small number of parameters.

1.5.1 Black hole thermodynamics

It was also discovered that black holes satisfy laws closely resembling the laws of thermodynamics [16, 17, 18]. The zeroth law is contained in the statement that the surface gravity κ of a black hole is constant through the horizon, which is a surprising result. First law of thermodynamics of black holes can be then written in the form

$$\delta M = \frac{\kappa}{8\pi}\,\delta A + \Omega\,\delta J + \Phi\,\delta Q, \tag{1.23}$$

where M is the mass of a black hole, A is the area of the horizon, Ω is the angular velocity of the horizon, J is the angular momentum of a black hole, Q and Φ are the charge and electrostatic potential, respectively (this equation excludes the magnetic charge, as it has yet not been discovered, if it actually exists in our Universe). (1.23) suggests that the surface gravity should be interpreted as the temperature of a black hole, area A as its entropy and remaining terms represent the work. This analogy is further supported by Hawking's discovery of the area law [19] that the area of an event horizon cannot decrease,

$$\delta A \geq 0; \tag{1.24}$$

clearly, the area law is analogous to the second law of thermodynamics if we identify the area with the entropy.

Even the third law of thermodynamics has its analogy in black hole physics. For a rotating black hole, its surface gravity decreases with the angular velocity and reaches zero for a certain value of angular momentum, in the case of the most usual Kerr metric this happens for value $J = M^2$. Such black holes are called *extremal* and the inner and outer horizons coincide. Extremal black holes have several interesting properties, for example they behave like superconductors [20, 21] and independently of external spacetime they have always geometry isometric

to Kerr-Newman black hole [22]. It was conjectured by Penrose [23] that for realistic matter there are no naked singularities, i.e. singularities must be always hidden under the horizon. Consequently, black holes cannot be super-extremal, they cannot rotate faster than extremal black holes because in such case there would be no horizons.

The third law of thermodynamics asserts that no physical process can produce an extremal black hole from black hole which was originally under-extremal. Since extremal black holes have vanishing surface gravity and, hence, vanishing temperature, this law of black hole physics again resembles the law that zero temperature cannot be achieved.

Thus, there seems to be a very close analogy between black hole laws and laws of thermodynamics. This is surprising, because thermodynamics is a phenomenological theory while laws of black hole mechanics are exact mathematical consequences of Einstein's equations. Therefore the analogy could be just accidental and misleading. Moreover, the first law (1.23) does not fix the relations surface gravity-temperature and area-entropy completely, it does so only up to proportionality factor. However, it was argued by Bekenstein [24] by thought experiments and dimensional arguements that entropy of a black corresponds to the loss of information about the matter that formed a black hole. Moreover, he argued that this entropy has quantum origin.

1.5.2 Hawking radiation

These arguments were fully justified by discovery of Hawking radiation [25]. Using the techniques of quantum field theory in curved spacetimes applied to spherically symmetric gravitational collapse he was able to show that an observer far from the black hole sees a thermal radiation with Planckian black-body spectrum (possibly corrected by a grey-body factor). Even before it was known that quantum effects on curved backgrounds typically lead to particle production, for example, in expanding universe [26]. The reason is that each observer must employ a set of creation/annihilation operators in terms of he defines the vacuum state. Say that a_k, b_k are annihilation operators of particles with momentum k associated with the two observers and $a_k^\dagger, b_k^\dagger$ are corresponding creation operators. Then vacuum states of both observers are defined by relations

$$a_k \left|0\right\rangle_A = 0, \qquad\qquad b_k \left|0\right\rangle_B = 0. \tag{1.25}$$

Expected number of particles with momentum k in a generic state $\left|\psi\right\rangle$ is then, for each observer,

$$N_A(k) = \left\langle\psi\right| a_k^\dagger \, a_k \left|\psi\right\rangle, \qquad N_B(k) = \left\langle\psi\right| b_k^\dagger \, b_k \left|\psi\right\rangle, \tag{1.26}$$

where $a_k^\dagger a_k$ has the meaning of the operator of number of particles. Different observers use different coordinate systems. In quantum field theory one starts with the classsical field equation, for example the wave equation

$$\Box\phi = 0. \tag{1.27}$$

Next step is to find an orthonormal basis u_k for the solutions of the wave equation such that the quantum field (now regarded as the operator) can be expanded into

the Fourier series

$$\phi(x) = \sum_k \left(a_k \, u_k(x) + a_k^\dagger \, u_k^*(x) \right) . \tag{1.28}$$

Observer in different frame will obtain similar expansion but with different basis resulting in different creation/annihilation operators. In fact, the relation between the two sets will be, in general, given by the so-called *Bogolyubov transformation* [27] of the form

$$a_k = \sum_q \left(\alpha_{kq} \, b_q + \beta_{kq} \, b_q^\dagger \right) . \tag{1.29}$$

In other words, the annihilation operator a_k is a mixture of both ladder operators of the observer B. Simple calculation shows that expected number of particles with momentum k in the vacuum state of observer B is

$${}_B\langle 0| \, a_k^\dagger a_k \, |0\rangle_B = \sum_q |\beta_{kq}|^2 . \tag{1.30}$$

Hence, what is a vacuum state for observer B is a non-vacuum state for observer A unless all coefficients b_{kq} in transformation (1.29) vanish.

This happens for inertial observers in Minkowski spacetime where the modes u_k are related by simple Lorentz transformation which preserves splitting of the field into negative and positive frequencies. In general, though, coefficients b_{kq} are non-vanishing. This is the mechanism behind the Hawking radiation but even in Minkowski spacetime an accelerated observer sees a thermal, so-called Unruh radiation [28].

Thus, it is not surprising that, in dynamical spacetime representing a gravitational collapse, quantum effects produce particles. The surprising result is the thermal character of the Hawking radiation and that this radiation is observable forever after the collapse. Quantum field theory in curved spacetimes is an approximate theory because it does not take into account the backreaction of quantum fields on the geometry. Therefore, if the Hawking radiation is present for all the time, its energy must be attributed to the energy loss of the black hole itself: black hole must evaporate in time. Hawking effect has been derived in many ways. More physical interpretation using quantum tunneling has been provided in [29], derivation using Feynman path integrals was given in [30]. Another interesting approach was employed in [31] where Gibbons and Hawking consider periodicity of Green functions in complexified time. However, there are also objections against the real existence of Hawking radiation, see e.g. [32].

1.5.3 Information paradox

The evaporation of black holes leads immediately to the so-called *information paradox* first pointed out by Hawking [33]. The essence of the paradox is the following. In quantum mechanics, the evolution is unitary so that if the system starts in a pure state $|\psi_0\rangle$, there is a unitary operator $U(t) = \exp(-i\,t\,H)$ (where H is the Hamiltonian) such that the state at arbitrary time is given by

$$|\psi(t)\rangle = U(t) \, |\psi_0\rangle = e^{-i\,t\,H} \, |\psi_0\rangle . \tag{1.31}$$

Operator $U(t)$ is invertible and hence the initial state vector $|\psi_0\rangle$ can be reconstructed from later state by

$$|\psi_0\rangle = U(-t)\,|\psi(t)\rangle = e^{i\,t\,H}\,|\psi(t)\rangle\,. \tag{1.32}$$

On the other hand, Hawking radiation is in thermal state and therefore it is describe by a density matrix rather than by a pure ket-state. Hence, apparently, during the black hole evaporation, collapsing matter which is initially in a pure state and caries a lot of bits of information undergoes a non-unitary evolution, ending in a mixed state characterized by few parameters. Although some physicists (and originally also Hawking) argue that information can be truly lost in the presence of gravity, other consider the conservation of information to be one of the most basic principles of physics, sometimes even called the -1st law of thermodynamics.

The whole situation can be nicely described in terms of Penrose diagrams. Consider standard spherical collapse visualised in figure 1.2. Penrose diagrams are not isometric to original spacetimes, rather they are conformally compactified [34]. That is, metric of a compactified spacetime g_{ab} is related to the metric of original spacetime $\tilde{g}_{ab}$ by conformal rescaling

$$g_{ab} = \Omega^2\,\tilde{g}_{ab}, \tag{1.33}$$

where Ω is an appropriately chosen conformal factor which vanishes at infinity. This infinity is represented by null hypersurfaces called *past null infinity* $\mathcal{I}^-$ and *future null infinity* $\mathcal{I}^+$. Since the spacetime is spherically symmetric, each point of the diagram is in fact a 2-sphere, except for the intersection i^0 called *spatial infinity* which is in fact only a single point: the origin of a null cone given by $\mathcal{I}^- \cup \mathcal{I}^+$. As we mentioned, conformal rescalings are not isometries, but they preserve the causal structure of the spacetime which means that the light cones in Penrose diagrams are represented by straight lines with the slope 45°. Shaded region in figure 1.2 represents collapsing matter, and $\mathcal{H}$ is another null hypersurface, namely the event horizon of the black hole. Finally, the zig-zag line represents the singularity of black hole. Since this singularity is spacelike, it is clear from the diagram that all causal curves crossing the horizon will inevitably end up in a singularity.

Now, the *predictability* means that the full spacetime can be reconstructed from the initial data given either on spacelike initial hypersurfaces (the Cauchy problem) or on null hypersurface (characteristic initial value problem). It has been shown that both such formulations of general relativity are well-posed, see [18, 35] and references therein. See also [13, 36] for rigorous treatment of causal structure of spacetime.

If the information is conserved during the collapse, the initial data should be recoverable from the final data. Obviously, observer at $\mathcal{I}^+$ cannot reconstruct the initial data on $\mathcal{I}^-$ because no geodesics from the interior of the black hole (and thus no information) will reach $\mathcal{I}^+$. In order to have a well-posed characteristic problem one needs to prescribe the data on $\mathcal{H} \cup \mathcal{I}^+$. Data given on the horizon would consist of information about the matter which crossed the horizon since the creation of the horizon. Classically, this is in principle possible. For example, a stationary observer just above the horizon could send the information about infalling matter to observer at $\mathcal{I}^+$. However, Hawking argued [33] that as soon

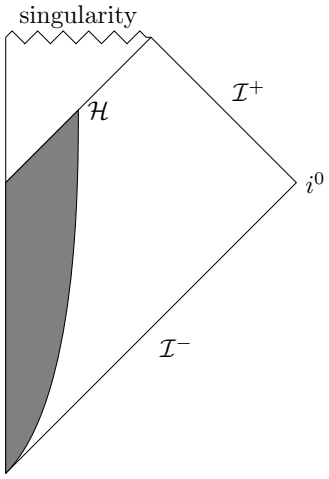

Figure 1.2: Spherical collapse according to classical general relativity.

as quantum effects are taken into account, namely the uncertainty principle, this is not viable. The basic heuristic argument is that in order to signal the time at which given particle crossed horizon would require energy of the same order as the energy of infalling particle. Hence, in order to provide the information about all infalling particles would require the same energy as the energy of matter that collapsed: hence there would be no energy left to even form a black hole.

In the case of evaporating black hole the Penrose diagram Fig. 1.2 must be modified. Following arguments are taken from [37] but there are also different approaches to the construction of Penrose diagrams for evaporating black holes, see e.g. [38].

Consider Penrose diagram Fig. 1.3 for evaporating black hole. Again, there is a zig-zag line representing the singularity but as the black hole evaporates, singularity disappears in a finite time and all the mass of the black hole is radiated through the Hawking radiation represented by a curly line emanating from point P. Let us analyze this process from the point of view of the Cauchy initial value problem. Suppose that the initial data are given on the initial hypersurface Σ before the collapse of the matter and formation of the black hole. That is, Σ contains full information about the spacetime and describes the matter in pure quantum state $|\Psi(\Sigma)\rangle$. Now consider later hypersurface $\Sigma_P = \Sigma_1 \cap \Sigma_2$ that contains a point P – intersection of the event horizon and the curvature singularity. Since the part Σ_1 lies inside the black hole, the Hilbert of states on Σ_P can be written as a direct product

$$\mathcal{H} = \mathcal{H}_1 \otimes \mathcal{H}_2. \tag{1.34}$$

Finally, there is a Cauchy hypersurface Σ' after the black hole has been fully evaporated and with this hypersurface we associate a pure state (assuming unitary evolution) $|\Psi(\Sigma')\rangle$. However, since Σ' is not causally connected to Σ_1, the full information present on Σ' had to be present already on Σ_2 and therefore the state on Σ_P had to be of the form

$$|\Psi(\Sigma_P)\rangle = |\Phi(\Sigma_1)\rangle \otimes |\chi(\Sigma_2)\rangle\,. \tag{1.35}$$

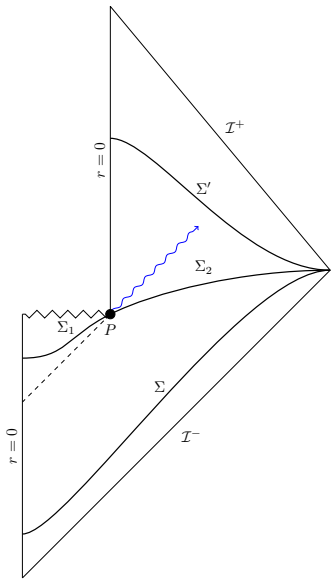

Figure 1.3: Conformal diagram for evaporating black hole and initial value problem. (Adopted from [37].)

Since states on Σ' are fully determined by states on Σ or, equivalently, Σ_2, and states on Σ_1 do not affect states on Σ_2 at all, states on Σ_1 must be completely independent on the initial state. In other words, information about the microstates of the matter is destroyed after the infalling matter crosses the horizon. On the other hand, according to the equivalence principle, nothing special happens to matter crossing the horizon and the previous conclusion therefore violates the equivalence principle. Apparently the only resolution of the paradox is that the observer at Σ' cannot see a pure state but a mixed state and hence the information contained in the initial was truly lost.

1.5.4 Black hole complementarity

Susskind et al [37] suggested that this apparent contradiction of basic principles can be resolved by the paradigm of *black hole complementarity* using the notion of *stretched horizon*. Using thermodynamical methods in quantum field theory it is possible to show [3] that the entropy of a quantum field outside the black hole horizon (subject to periodic boundary conditions) is given by

$$S \propto \int |\log k\,\epsilon|\,\mathrm{d}k, \tag{1.36}$$

where ϵ is a proper distance from the black hole horizon and represents a cut-off necessary to regularize the integral. It order to recover Bekenstein-Hawking temperature and entropy, ϵ must be of order of the Planck length ℓ_P. The stretched horizon is then introduced as a spacelike surface whose radius is $2M + \epsilon$, i.e. the Schwarzschild radius increased by the Planck length. Being spacelike rather than null, stretched horizon admits physical processes to happen on it. In fact, it behaves like a hot membrane with electric and thermodynamic properties.

The notion of entanglement entropy and its relation to 2nd law of thermodynamics and equivalence principle was already discussed. Another ingredient

crucial for the black hole complementarity is the so-called *no-cloning principle* saying that no device can accept a quantum state on its input and produce the original state and its duplicate on the output [39]. Among others, that would violate the Heisenberg uncertainty principle because one would be able to do incompatible measurements on exactly the same systems. Suppose that such cloning device $\mathcal{C}$ exists. Acting on the spin states it produce

$$\mathcal{C} : |\uparrow\rangle \mapsto |\uparrow\rangle \otimes |\uparrow\rangle\,, \qquad \mathcal{C} : |\downarrow\rangle \mapsto |\downarrow\rangle \otimes |\downarrow\rangle\,, \tag{1.37}$$

Now suppose that we insert a superposed state

$$|\psi\rangle = \frac{1}{\sqrt{2}}\left(|\uparrow\rangle + |\downarrow\rangle\right), \tag{1.38}$$

so that

$$\begin{aligned}\mathcal{C} : |\psi\rangle &\mapsto \frac{1}{2}\left(|\uparrow\rangle + |\downarrow\rangle\right) \otimes \left(|\uparrow\rangle + |\downarrow\rangle\right) \\ &= \frac{1}{2}\left(|\uparrow\rangle \otimes |\uparrow\rangle + |\uparrow\rangle \otimes |\downarrow\rangle + |\downarrow\rangle \otimes |\uparrow\rangle + |\downarrow\rangle \otimes |\downarrow\rangle\right).\end{aligned}$$

On the other hand, by linearity, we have

$$\mathcal{C} : |\psi\rangle = \frac{1}{\sqrt{2}}\left(|\uparrow\rangle \otimes |\uparrow\rangle + |\downarrow\rangle \otimes |\downarrow\rangle\right). \tag{1.39}$$

Hence, we got two contradictory results and thus the existence of device $\mathcal{C}$ is impossible.

The no-cloning theorem has important implications for the Penrose diagram 1.3. We have argued that states on Σ_1 do not carry information about the infalling matter. Now we see the reason: any information about infalling matter present on Σ. If the final state on Σ' is pure, all information on Σ must be present also on Σ_2. The no-cloning theorem shows that the same information cannot be simultaneously stored on Σ_1 because it would require copying the quantum information which, as we have now seen, is forbidden.

On the other hand, black holes have entropy $S = A/4$ and entropy is related to the dimensionality of underlying Hilbert space via

$$\dim \mathcal{H} = e^S. \tag{1.40}$$

Assuming still the unitary evolution, although the Hawking radiation appears to be thermal, it must carry the information about the infalling matter through subtle correlations between Hawking photons and degrees of freedom of the black hole. Hence, as black hole evaporates, the information will slowly leak from the black hole.

Although the stretched horizon is a real physical membrane, respecting the principle of equivalence, a freely falling observer will notice anything unusual when crossing the event horizon. Physical properties of the stretched horizon can be measured by a stationary observer close to the horizon. The idea of black hole complementarity is that there is no contradiction in these two points of view. First, it is clear that the outside observer cannot receive signals from the infalling observer and therefore cannot get a message saying that there is no hot membrane. What *can* in principle happen is the following.

1.6 Bekenstein limit

Content of this section is heavily inspired by [2] by Horacio Cassini. Bekenstein limit is a remarkable result first formulated by Jacob D. Bekenstein in [40] and later reformulated in a covariant form in [41]. It posits an upper bound on the entropy of some region of spacetime as

$$S \leq \lambda ER, \tag{1.41}$$

where λ is some real number of order $\mathcal{O}(1)$, E is the energy contained in the region and R is the region's typical size. In the original paper it was developed through thought experiment considering thermodynamics and relativity.

In [2] this bound is shown to be somewhat ill-defined as from the point of view of QFT it is not obvious how to interpret the involved quantities. Just directly restricting the defining domains does not work as it can be shown that, for example, from spatially localized states with energy E_0 a state with any energy lower than E_0 can be superposed. This fact then implies, that localized states with given energy do not form a vector space and do not have defined entropy. On the other hand, energy and entropy is well defined for a global state, but then the question raises, what does the value R represent in such a case. Also, there is some disagreement over the actual value of the parameter λ.

The problem can be resolved with slight redefinition of the energy and entropy. Assume a discretized quantum system, whose state is represented with the density operator $\hat{\rho}$. Restriction to the points inside a volume V can be done by tracing over the states occupying the exterior of the volume, symbolically

$$\hat{\rho}_V = \mathrm{Tr}_{\mathcal{C}(V)}\, \hat{\rho}. \tag{1.42}$$

We can now assign the entropy to this state as usual,

$$S(\hat{\rho}) = -\,\mathrm{Tr}_V\, \hat{\rho}_V \ln(\hat{\rho}_V), \tag{1.43}$$

but this is shown to be divergent in the limit of vanishing distances between the points of the system (namely for such cutoff ϵ the entropy diverges as ϵ^{-2}). The correct way to circumvent this problem is argued to be the subtraction of the vacuum entropy from the entropy in (1.43), explicitly

$$S_V(\hat{\rho}) = S(\hat{\rho}_V) - S(\hat{\rho}^0_V), \tag{1.44}$$

where $\hat{\rho}^0$ corresponds to the complete vacuum state (and, when localized, describes the vacuum fluctuations). As the divergence in $S(\hat{\rho})$ is independent of $\hat{\rho}$, it is the same for the vacuum state and so after the subtraction only the finite part remains.

In [2] it is further shown that the same approach can be deployed to make sense of the RHS of the inequality (1.41). The product λER is expressed by the means of the modular Hamiltonian K for volume V, which is implicitly defined as

$$\rho^0_V = \frac{e^{-K}}{\mathrm{Tr}_V\, e^{-K}}. \tag{1.45}$$

Also the discussion of parameter λ is made, showing, that it depends on the volume V, into which we localize the state, most commonly having the value of 2π, π and similar. The actual expression of the RHS is (choosing $\lambda = 2\pi$ as this corresponds to the common case of V being a sphere)

$$\lambda ER = \mathrm{Tr}_V(K\rho_V) - \mathrm{Tr}_V(K\rho_V^0) \tag{1.46}$$

where the similarity to (1.44) is obvious and the reasoning for the subtraction is also similar, to eliminate the divergent quantities.

It is to stress that all the reasoning in this section was based on quantum theory considerations. If we now replace the quantities in (1.41) with the newly defined ones from (1.44) and (1.46), we acquire

$$\begin{aligned} S(\hat{\rho}_V) - S(\hat{\rho}_V^0) &= \mathrm{Tr}_V\, \hat{\rho}_V^0 \ln\left(\hat{\rho}_V^0\right) - \mathrm{Tr}_V\, \hat{\rho}_V \ln(\hat{\rho}_V) \leq \\ \leq \mathrm{Tr}_V(K\rho_V) - \mathrm{Tr}_V(K\rho_V^0) &= \mathrm{Tr}_V\, \hat{\rho}_V^0 \ln\left(\hat{\rho}_V^0\right) - \mathrm{Tr}_V\, \hat{\rho}_V \ln\left(\hat{\rho}_V^0\right) \\ \implies 0 \leq \mathrm{Tr}\, \hat{\rho}_V(\ln(\hat{\rho}_V) - \ln\left(\hat{\rho}_V^0\right)) &= S(\hat{\rho}_V|\hat{\rho}_V^0) \end{aligned} \tag{1.47}$$

where $S(\hat{\rho}_V|\hat{\rho}_V^0)$ coincides with the definition of the relative entropy. It is easy to check, that the relative entropy is always greater than zero (exploiting the property of logarithm $\ln(1+x) \leq x$) and so this inequality must hold always. And so the improved Bekenstein bound must be true only from reasoning on the quantum level. When we recall, that the bound was originally conceived from relativistic considerations, it can support the conjecture, that quantum theory might be more fundamental than relativity.

1.7 Page curve

Let us take a point of view that the collapse of a matter in pure state, evaporation of a black hole and ultimate disappearance of a singularity (cf. Fig. 1.3) is a unitary process so that it can be regarded as a scattering quantum process given by an S-matrix connecting data on past and future null infinity. Next, assume that the Bekenstein limit implies the finite dimension of the underlying Hilbert space.

Based on these assumptions, Page in his seminal papers [42, 43] formulated a paradigm of unitary black hole evaporation. It is not a microscopic model but a phenomenological description of black hole evaporation. Assume that the Hilbert space can be factorized as

$$\mathcal{H} = \mathcal{H}_1^p \otimes \mathcal{H}_2^q, \qquad \dim \mathcal{H} = N \equiv p\, q, \tag{1.48}$$

where the subsystem $\mathcal{H}_1^p$ of dimension p describes the degrees of freedom of the black hole itelsf and subsystem $\mathcal{H}^q$ represents the states of the Hawking radiation. During the evaporation, the whole system is always in the pure state but entangled state so that the Hawking radiation as a subsystem is described only in terms of the density matrix. At the beginning of evaporation, immediately after the formation of a black hole, $q = 1$ since there is no Hawking radiation

outside the black hole and corresponding Hilbert space is one dimensional (only a vacuum state):

$$|\Psi_0\rangle = |\psi_0\rangle \otimes |0\rangle \,. \tag{1.49}$$

Such state is by definition disentangled and the von Neuman entropy is zero. As the black hole starts to evaporate, dimensionality q increases and p decreases, keeping $N = p\,q$ constant and we have general entangled state

$$|\Psi\rangle = \sum_{I,n} |I\rangle \otimes |n\rangle \,. \tag{1.50}$$

The question is what is expected entropy or, in other words, expected information hidden in the correlactions between black hole and Hawking radiation. Since we do not know underlying micrsoscopic dynamics, the best estimate is to calculate the average value of entropy for all possible states. Select an arbitrary but fixed state $|\Psi_0\rangle$ and generate a random unitary matrix U with uniform distribution. Then,

$$U\,|\Psi\rangle_0 \tag{1.51}$$

is a uniformly generated random state in $\mathcal{H}$. Averaging through all unitary matrices U with the de Haar measure one finds an expected value of the entropy. Page conjectured, and it was later proven in [44], that the mutual information between the two subsystems is

$$I_{p,q} = \ln p + \frac{p-1}{2\,q} - \sum_{k=q+1}^{p} q\frac{1}{k}. \tag{1.52}$$

At the end of the evaporation, black hole disappears and only Hawking radiation remains, so that the final state is of the form

$$|\Psi_{\text{fin.}}\rangle = |0\rangle \otimes |N\rangle \,. \tag{1.53}$$

This state is again disentangled and hence the final entropy is zero again, leading to a pure state of the Hawking radiation. This paradigm is demonstrated on the so-called *Page curve*, see Fig. 1.4.

1.8 Quasi-particle picture and the emergence

In paper by Acquaviva, Iorio and Scholtz [45] another lines of reasoning have been pursued in order to support the idea of emergence of gravity from more fundamental micsroscopic degrees of freedom. The two essential inputs are

1. Bekenstein-Hawking entropy interpreted as the (logarithm) of the dimension of underlying Hilbert space;

2. analogies of emergence of geometry in condensed matter physics.

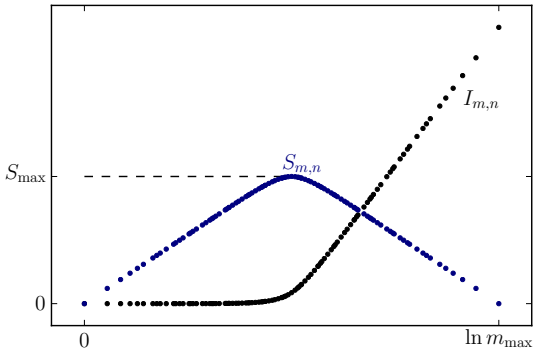

Figure 1.4: Page curve demonstrating the unitary evolution during black hole evaporation. (Adopted from [45])

There are several arguments in the favor of the first statement, see also [7]. The other claim is motivated especially by graphene layers in which new effective types of geometries can arise as a consequence of the interactions of the lattice with free electrons. For example, such electrons behave like quanta of massless Dirac field on curved background which has interesting consequences: existence of horizons, analogies of Hawking or Unruh radiation. See for example reviews [46, 47, 48].

In [45] it is first qualitatively argued that both geometries and quantum fields should emerge from the same Hilbert space whose dimensionality is given by the Bekenstein limit. Then, a simplistic kinematical model á la Page is constructed. Instead of simple factorization into two subsystems, the authors considered the direct sum of such factorization and each term in the sum represents different rearrangement of degrees of freedom between geometrical and field part. In analogy with condensed matter physics, where different lattice structures can lead to same effective geometries, even though the spacetime is flat after the black hole evaporates, on microscopic level the arrangement can be different than before the creation of black hole. Hence, instead of simple factorization it is necessary to use a graph structure

$$\mathcal{H} = \bigoplus_i T_i, \qquad \text{where} \qquad T_i = \mathcal{H}_1^{p_i} \otimes \mathcal{H}_2^{q_i}. \tag{1.54}$$

We call T_i the topologies of the graph and each topology has a form a direct product of degrees of freedom of geometry and those of the matter. Then, using the Page approach, i.e. by averaging over all possible states, it was shown that after black hole evaporates, on average there is a resdiual entanglement between the two subsystems – black hole is gone but there are still some degrees of freedom forming the background geometry. Hence, the final entropy is not zero and the Hawking radiation is still in a mixed state. This was numerically demonstrated in [45], see Fig. 1.5.

However, all these models are phenomenological, they lack exact mechanism how the process of evaporation really takes place. There are attempts to construct such exact models in lower-dimensional spacetimes where conformal symmetries constrain the dynamics significantly. Such models typically represent low energy limits of stringy black holes, see, e.g. [49]. In this thesis we turn to different class of models that closely follow ideas introduced in [45, 7] and study a specific model

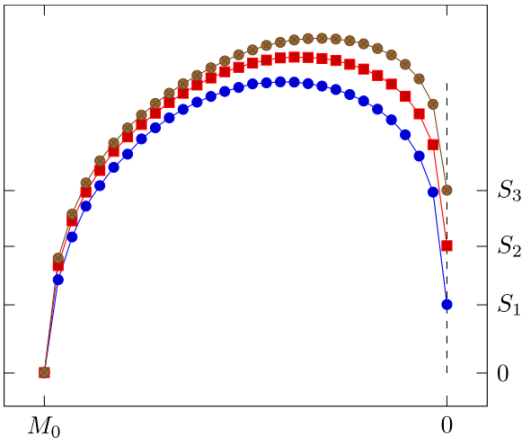

Figure 1.5: Deviations from the expected Page curve for a quasi-particle picture of spacetime emergence. Different curves correspond to different choices of dimensionalities of Hilbert spaces and each curve represents a system consisting of two topologies. (Adopted from [45])

proposed in [6].

2. Computational methods

2.1 Exact embedding

In this section a short description follows on the process of embedding a metric space into an Euclidean one. Firstly a few notions are defined, such as the triple product and an n-simplex. Then it will be shown, how can an n-simplex be assigned its volume in the case of Euclidean space and what is the meaning of the volume in general metric space. Lastly the algorithm of embedding the metric space into an Euclidean one will be presented.

2.1.1 Triple product and volume

Let (X,d) be a fixed metric space (X is the set of points of the space and d is the distance function between those points), then for $x, y, z \in X$ we can define their triple product

$$\langle x,\, y,\, z\rangle = \frac{1}{2}((d(x,z))^2 + (d(y,z))^2 - (d(x,y))^2). \tag{2.1}$$

A set of $n+1$ points from the space X is called an n-simplex. Assume an n-simplex Y to which we want to assign its volume. Y can be also described by the set of the points it consist of as $Y = \{x_0,...,x_n\}$. Assume the set $\{x_0,...,x_n\}$ to be an ordered n+1-tuple of points. Then define

$$D(x_0,...,x_n) = \det(A_{ij}),\ \text{where } A_{ij} = \langle x_i,\, x_j,\, x_0\rangle;\ i,j \in \{1,...,n\}. \tag{2.2}$$

It can be shown that D is symmetric and on the set of simplices it acquires only real values. Also, under the assumption that X is a subset of an Euclidean space, the triple product corresponds to the scalar product via the relation

$$\langle x_i,\, x_j,\, x_0\rangle = (x_i - x_0)\cdot(x_j - x_0). \tag{2.3}$$

Another interesting fact which can be proven is that the square root of the determinant (2.2) for given simplex is equal to the volume of the parallelotope spanned by the vectors $\{x_1 - x_0,...,x_n - x_0\}$. To acquire the volume of the n-simplex, one needs to divide by $n!$, so

$$\mathrm{Vol}(Y) = \frac{1}{n!}\sqrt{D(x_0,...,x_n)}. \tag{2.4}$$

This formula will be used as a general mean of finding the volume of a simplex in the space X, regardless of whether it is a subset of Euclidean space or not. The downside to this is that the volume defined by (2.4) can acquire complex values for generic metric space X. In the special case of X such, that each n-simplex of X has real volume, the X will be called *flat*. If X is flat, than its *dimension* can be defined as the highest n, for which there exist an n-simplex of X with non-zero volume.

2.1.2 Embedding of an n-simplex

Let V be a real space with inner product (the inner product induces a metric). An *embedding* of X into V is then an isometry from X to V.

Theorem 2. *A metric space can be embedded in Euclidean n-space if and only if the metric space is flat and of dimension less than or equal to n.*

The full proof of this statement can be found in [50] but here only the tools to compute the embedding will be presented. Let (X,d) be flat metric space of dimension n (so all subsets of X consisting of $n+1$ points or less can be interpreted as simplices with positive volumes). Then one of the n-simplices with non-zero volume defined by points $\{x_0,...,x_n\}$ is picked, which will become a set of basis vectors of the embedding (namely the set $\{x_1 - x_0, x_2 - x_0,...,x_n - x_0\}$). Lastly the function

$$f(x) = (\langle x,x_1,x_0\rangle,\langle x,x_2,x_0\rangle,...,\langle x,x_n,x_0\rangle) \tag{2.5}$$

is defined, which takes as its argument points of X and assigns to them a set of n real numbers, which will be understood as their coordinates with respect to the basis given by the simplex $\{x_0,...,x_n\}$. In [50] it is also shown, that for vectors $\vec{u}, \vec{v}$ represented in the basis $\{x_1 - x_0, x_2 - x_0,...,x_n - x_0\}$ as numeric vectors u_L, v_L, it holds $(u,v) = u_L^T L^{-1} v_L$, where $L_{ij} = \langle x_i,x_j,x_0\rangle$. So if we find matrix R such, that $R^T R = L^{-1}$, than the representation of vectors $\vec{u}, \vec{v}$ in unit Euclidean basis will be $u_E = R \cdot u_L$ and $v_E = R \cdot v_L$.

The matrix R can be acquired for example by Cholesky Decomposition [51]. In most general case this is a decomposition of regular matrix A into two matrices R and $R^\dagger$, which satisfy $RR^\dagger = A$ (A can be generally hermitian, even though it is real in our case) and A is positive definite. The matrix R is a upper triangular matrix and can be iteratively found in finite number of steps as follows.

Assume an $n \times n$ matrix A and assign it a set of n matrices A_i such that

$$A_i = \begin{pmatrix} I_{i-1} & 0 & 0 \\ 0 & a_i & b_i \\ 0 & b_i^\dagger & B_i \end{pmatrix}, \tag{2.6}$$

where I_j denotes a j by j identity matrix, a_j is a scalar, b_j is a vector of j numbers and B_j is a general j by j matrix. Also choose $A_1 := A$. Now define

$$R_i = \begin{pmatrix} I_{i-1} & 0 & 0 \\ 0 & \sqrt{a_i} & \frac{b_i}{\sqrt{a_i}} \\ 0 & 0 & I_{n-1} \end{pmatrix} \tag{2.7}$$

Then it holds that $A_i = R_i\, A_{i+1}\, R_i^\dagger$, so, after n steps this results into $A = R_1 R_2 \dots R_n (R_1 R_2 \dots R_n)^\dagger$ and so the sought after decomposition $A = RR^\dagger$ satisfies $R = R_1 R_2 \dots R_n$.

2.2 Multidimensional scaling

Multidimensional scaling was developed as a data visualisation method. Having a set of objects and a weight for each pair from this set (which is commonly

referred to as the distance) the MDS tries to embed the objects into a flat Euclidean space of some dimension. The dimension is found by construction and investigation of the resulting embedding coordinates. Sometimes the points do not fit exactly into a flat space and there is some discrepancy between the initial data and the resulting embedding. The most common way to describe this is the stress function, which is defined below.

On the historical note, according to [52] this method was originally created for psychologists working with data acquired mostly by letting subject evaluate relations between some stimuli (e.g. how similar of different are two given pictures). Output of such survey is only a table of these evaluations of given relation, averaged over all the subjects. While some structure can be seen from this format of the data, MDS can provide very nice visualisation. The value lies in the fact that there is often some additional information about the data being studied and one can then find (e.g. from the distances between the point in the MDS embedding) numerical description for phenomena otherwise hard to quantify. It is to note that we do not have any additional information and only seek to embed a set of points with given distances into flat space as good as possible.

To understand the computation itself a reverse approach is employed, as can be seen in [6]. Imagine we already have the embedding coordinates. Let us put all vectors corresponding to coordinates of individual points into one matrix X, whose n-th row are the coordinates of the n-th point and the d-th column corresponds to the distance in d-th dimension. X is of dimensions $N \times D$ and of the rank at most D as $D \leq N$. Now define matrix

$$B = XX^T \implies B_{pq} = \sum_{r=1}^{D} X_{pr} X_{qr}, \tag{2.8}$$

which is a $N \times N$ matrix but still of the same rank as X. It is to note, that the definition of B is unambiguous up to an orthonormal transform $X' = XO$.

If a number is assigned to each point according to the row with its coordinates in X, than distance between points p and q can be expressed as

$$d(p,q)^2 = \sum_{r=1}^{D} (X_{pr} - X_{qr})^2 = \sum_{r=1}^{D} X_{pr}^2 + X_{qr}^2 - 2X_{pr}X_{qr} = B_{pp} + B_{qq} - 2B_{pq}. \tag{2.9}$$

Adding an additional condition that the coordinates are centred at the origin

$$\sum_{p=1}^{D} X_{pr} = 0 \qquad \forall r \tag{2.10}$$

and substituting

$$\sum_{p=1}^{N} d(p,q)^2 = NB_{qq} + \sum_{p=1}^{N} B_{pp} \text{ and } \sum_{p,q=1}^{N} d(p,q)^2 = 2N \sum_{p=1}^{N} B_{pp} \tag{2.11}$$

into (2.9) we get

$$B_{pq} = \frac{1}{2} \left(-d(p,q)^2 + \frac{1}{N} \sum_{k=1}^{N} d(k,q)^2 + \frac{1}{N} \sum_{k=1}^{N} d(p,k)^2 - \frac{1}{N^2} \sum_{k,l=1}^{2} d(k,l)^2 \right). \tag{2.12}$$

It is to note that while the matrix X was used in the reasoning, up to now it was not actually computed and it is obvious from (2.12) that matrix B can be acquired only from the distances between the points. The next step is to diagonalize B and do the following decomposition:

$$B = R\Lambda R^T = (R\sqrt{\Lambda})(R\sqrt{\Lambda})^T \tag{2.13}$$

where R is appropriate $N \times N$ matrix so that $\Lambda = \mathrm{diag}(\lambda_1, \ldots, \lambda_N)$ is diagonal and $\sqrt{\Lambda} = \mathrm{diag}(\sqrt{\lambda_1}, \ldots, \sqrt{\lambda_N})$. As B was only of rank D, among the numbers λ_j there will be only D nonzero values. Assuming that those are the first D numbers on the diagonal of $\sqrt{\Lambda}$, we can identify the first D columns of $R\sqrt{\Lambda}$ as X:

$$(R\sqrt{\Lambda})_{kl} = X_{kl} \text{ for } k \in \{1, \ldots, N\},\ l \in \{1, \ldots, D\} \tag{2.14}$$

while keeping on mind the uniqueness up to an orthonormal transform. The omitted $N - D$ columns of $R\sqrt{\Lambda}$ are zero so no information was lost.

In the case that exact embedding into flat space is not possible it might be that the distortion from flatness is only small and at least an approximate embedding can be found. If this is the case there are D large nonzero eigenvalues of B $\{\lambda_1, \ldots, \lambda_D\}$ while the rest of the λ's can be nonzero too, but of much smaller magnitude than the former . The function proposed in [6] to assess, if the distortion from flat space is small enough, is

$$\epsilon_D = 1 - \frac{\sum_{i=1}^{D} |\lambda_i|}{\sum_{i=j}^{N} |\lambda_j|} \tag{2.15}$$

where 0 means no distortion and 1 maximal.

2.3 Density matrix and its tracing

Assume a quantum system specified by a state $|\Psi\rangle$ from the Hilbert space $\mathscr{H}$, which can be expanded with respect to some orthonormal basis as

$$|\Psi\rangle = \sum_I c_I |\phi_I\rangle , \tag{2.16}$$

where I is a general index set. If the system under investigation consists of several independent subsystems, the total Hilbert space can be decomposed into appropriate subspaces, each corresponding to one of these subsystems,

$$\mathscr{H} = \bigotimes_{i=1}^{S} \mathscr{H}_i,$$

where S is the number of subsystems. So the state $|\Psi\rangle$ can be expressed as

$$|\Psi\rangle = \sum_{m,\ldots,n=1}^{N_m,\ldots,N_n} c_{m\ldots n} |\phi_m\rangle \otimes \cdots \otimes |\phi_n\rangle , \tag{2.17}$$

where the number of indices $m \ldots n$ is S and they span all the basis vectors from an arbitrary chosen basis on a Hilbert subspaces $\mathscr{H}_i$ and so $\dim \mathscr{H}_m = N_m$ and $\dim \mathscr{H} = \prod_{i=1}^{S} N_i$.

Now assume an operator $\hat{A}$, which acts on $\mathscr{H}$. The projection of the complete state $|\phi\rangle$ from $\mathscr{H}$ onto its i-th subspace $\mathscr{H}_i$ is specified by the i-th ket in the tensor product decomposition $|\phi\rangle = |\phi_m\rangle \otimes \ldots \otimes |\phi_n\rangle$. Then $\hat{A}$ can be expanded with respect to the basis $\{|\phi_m\rangle \otimes \ldots \otimes |\phi_n\rangle\}_{m,\ldots,n=1}^{N_m,\ldots,N_m}$ as

$$\hat{A} = \sum_{m,\ldots,n=1}^{N_m,\ldots,N_n} \sum_{m',\ldots,n'=1}^{N_{m'},\ldots,N_{n'}} a_{m\ldots nm'\ldots n'} \, |\phi_m\rangle \otimes \ldots \otimes |\phi_n\rangle \, \langle\phi_{m'}| \otimes \ldots \otimes \langle\phi_{n'}| \tag{2.18}$$

with the notational convention that $|a\rangle|b\rangle = |a\rangle \otimes |b\rangle$ and $\langle a|\langle b| \cdot |c\rangle|d\rangle = \langle a|c\rangle \, \langle b|d\rangle$.

Focusing on the mean value of $\hat{A}$ in the state $|\Psi\rangle$ it can be seen, that [3]

$$\begin{aligned}
\langle\hat{A}\rangle_{|\Psi\rangle} &= \sum_{M,M'} c^*_{m\ldots n} c_{m'\ldots n'} \, \langle\phi_m| \ldots \langle\phi_n| \, \hat{A} \, |\phi_{m'}\rangle \ldots |\phi_{n'}\rangle = \\
&= \sum_{M,M',J,J'} c^*_{m\ldots n} c_{m'\ldots n'} a_{j\ldots kj'\ldots k'} \, \langle\phi_m| \ldots \langle\phi_n|\phi_j\rangle \ldots |\phi_k\rangle \cdot \\
&\qquad \cdot \langle\phi_{j'}| \ldots \langle\phi_{k'}|\phi_{m'}\rangle \ldots |\phi_{n'}\rangle = \\
&= \sum_{M,M',J,J',S} c^*_{m\ldots n} c_{m'\ldots n'} a_{j\ldots kj'\ldots k'} \, \langle\phi_m| \ldots \langle\phi_n|\phi_s\rangle \ldots |\phi_t\rangle \cdot \\
&\qquad \cdot \langle\phi_s| \ldots \langle\phi_t|\phi_j\rangle \ldots |\phi_k\rangle\langle\phi_{j'}| \ldots \langle\phi_{k'}|\phi_{m'}\rangle \ldots |\phi_{n'}\rangle = \\
&= \sum_S \langle\phi_s| \ldots \langle\phi_t| \sum_{M,M'} c^*_{m\ldots n} c_{m'\ldots n'} \, |\phi_{m'}\rangle \ldots |\phi_{n'}\rangle\langle\phi_m| \ldots \langle\phi_n| \cdot \\
&\qquad \cdot \sum_{J,J'} a_{j\ldots kj'\ldots k'} \, |\phi_j\rangle \ldots |\phi_k\rangle\langle\phi_{j'}| \ldots \langle\phi_{k'}| \; |\phi_s\rangle \ldots |\phi_t\rangle = \\
&= \sum_S \langle\phi_s| \ldots \langle\phi_t| \, \hat{\rho}\hat{A} \, |\phi_s\rangle \ldots |\phi_t\rangle = \mathrm{Tr}(\hat{\rho}\hat{A}),
\end{aligned} \tag{2.19}$$

where the density operator $\hat{\rho}$ is defined as

$$\hat{\rho} = \sum_{M,M'} c^*_{m\ldots n} c_{m'\ldots n'} \, |\phi_{m'}\rangle \ldots |\phi_{n'}\rangle\langle\phi_m| \ldots \langle\phi_n| \tag{2.20}$$

To this operator a matrix can be assigned, it will be called the *density matrix*. Especially if expressed with respect to the basis $\{|\phi_m\rangle \ldots |\phi_n\rangle\}_{m,\ldots,n=1}^{N_m,\ldots,N_n}$, then its elements are $c^*_{m\ldots n} c_{m'\ldots n'}$. Also it is obvious, that $\hat{\rho} = |\psi\rangle\langle\psi|$. This is a general rule how to assign each pure state (pure as opposed to mixed) a density matrix.

Next notion defined will be the *reduced operator* (and corresponding *reduced matrix*). Assume that only two subsystems are interesting and in the set of indices $m \ldots n$ let the corresponding indices be e.g. i, j. Then the reduced operator is defined as being traced over the Hilbert space of all the objects but those two of interest, so

$$\hat{\rho}_{ij} = \sum_{M\setminus\{i,j\}} \langle\phi_m| \ldots \otimes \hat{\mathbb{1}}_i \otimes \ldots \otimes \hat{\mathbb{1}}_j \otimes \ldots \langle\phi_n| \, \hat{\rho} \, |\phi_m\rangle \ldots \otimes \hat{\mathbb{1}}_i \otimes \ldots \otimes \hat{\mathbb{1}}_j \otimes \ldots |\phi_n\rangle \,, \tag{2.21}$$

[3] From now on the upper limits of the summations will be omitted to avoid cluttering. Also in the equations the sets of indices like $m, \ldots, n$ by multi-indices named after the first letter in the set of indices, eg. $m, \ldots, n = M$

where the symbol $\hat{\mathbb{1}}_i$ stands for an identity operator on the space of i-th object and $\sum_{M\setminus\{i,j\}}$ sums over all indices $m,\ldots,n$ apart from i-th and j-th (and also the omitted upper limit of the summation would be missing the values corresponding to i and j). Inserting the definition of $\hat{\rho}$ into (2.21) then leads to

$$\begin{aligned}\hat{\rho}_{ij} = \sum_{M,M',S\setminus\{i,j\}} & c^*_{m\ldots n} c_{m'\ldots n'} \langle\phi_s| \ldots \otimes \hat{\mathbb{1}}_i \otimes \ldots \otimes \hat{\mathbb{1}}_j \otimes \ldots \langle\phi_t|\phi_{m'}\rangle \ldots |\phi_{n'}\rangle \cdot \\ & \cdot \langle\phi_m| \ldots \langle\phi_n|\phi_s\rangle \ldots \otimes \mathbb{1}_i \otimes \ldots \otimes \mathbb{1}_j \otimes \ldots |\phi_t\rangle = \\ = \sum_{M,M',S\setminus\{i,j\}} & c^*_{m\ldots n} c_{m'\ldots n'} \delta_{sm'} \ldots \delta_{tn'} \delta_{sm} \ldots \delta_{nt} \, |\phi_i\rangle|\phi_j\rangle\langle\phi_{i'}|\langle\phi_{j'}| = \ldots\end{aligned} \tag{2.22}$$

where among the Kronecker's delta symbols those corresponding to i-th and j-th position are missing twice, once for the primed and once for the unprimed indices m to n. Then the reduced operator can be simplified as

$$\ldots = \sum_{M,M'} c^*_{m\ldots n} c_{m'\ldots n'} \delta_{mm'} \ldots \delta_{nn'} \, |\phi_i\rangle|\phi_j\rangle\langle\phi_{i'}|\langle\phi_{j'}| = \tag{2.23}$$

$$= \sum_{M,i',j'} c^*_{m\ldots i\ldots j\ldots n} c_{m\ldots i'\ldots j'\ldots n} \, |\phi_i\rangle|\phi_j\rangle\langle\phi_{i'}|\langle\phi_{j'}| = \tag{2.24}$$

$$= \sum_{i,j,i',j'=1}^{N_i,N_j,N_{i'},N_{j'}} |\phi_i\rangle|\phi_j\rangle\langle\phi_{i'}|\langle\phi_{j'}| \sum_{M\setminus\{i,j\}} c^*_{m\ldots i\ldots j\ldots n} c_{m\ldots i'\ldots j'\ldots n} = \tag{2.25}$$

$$= \sum_{i,j,i',j'=1}^{N_i,N_j,N_{i'},N_{j'}} |\phi_i\rangle|\phi_j\rangle\langle\phi_{i'}|\langle\phi_{j'}| \, \rho_{iji'j'}. \tag{2.26}$$

and the numbers $\rho_{iji'j'}$ form the reduced matrix.

The notion of reduced matrix can be generalized to any number of objects, and thus indices, over which the original density operator is not traced, e.g.

$$\hat{\rho}_{q,\ldots,s} = \sum_{\{q,\ldots,s\}=1}^{\{N_q,\ldots,N_s\}} \rho_{q\ldots sq'\ldots s'} \, |\phi_q\rangle \ldots |\phi_s\rangle\langle\phi_{q'}| \ldots \langle\phi_{s'}| \tag{2.27}$$

where
$$\rho_{q\ldots sq'\ldots s'} = \sum_{M\setminus\{q,\ldots,s\}} c^*_{m\ldots q\ldots s\ldots n} c_{m\ldots q'\ldots s'\ldots n} \tag{2.28}$$

.

3. Results

3.1 Examples of embeddings

We have attempted numerical computation of embedding of a quantum state into some metric space. As there is little to none preceding calculations in this direction (we are aware of such computations for Heisenberg chain and Toric code in [6]), we have tried only simple states. This means that our results cannot be interpreted as some specific or known geometry yet. On the other hand a few interesting properties were found and they will be stressed at appropriate places. Also there is great space for development in the size of calculations. On commonly available personal computers it is possible to compute embedding of at most 22 points in a convenient time. To illustrate, assume that the Hilbert space corresponding to one point of embedding is 2-dimensional, than the complexity of the calculation approximately grows with the dimension of the total Hilbert space. This Hilbert space is taken to be the tensor product of N one-point Hilbert spaces and so its dimension is 2^N, which is exponentially growing. Despite serious effort, we were unable to lower the computational difficulty of this task.

In our case we assume a set of Hilbert spaces $\mathscr{H}$ of dimension 2 and want to interpret them as points of some emergent geometry. If we denote the basis of each such small Hilbert space $\{|0\rangle, |1\rangle\}$, then the basis of the total Hilbert space $\mathscr{H}_{tot}$ defined as a tensor product of N small spaces $\mathscr{H}_{tot} = \bigotimes_{i=1}^{N} \mathscr{H}_i$ can be naturally chosen as the tensor product of all possible combinations of $|0\rangle$'s and $|1\rangle$'s. Then we can easily express a state as the set of its coefficients with respect to this large basis. We have tried several states, out of which 7 have shown at least some interesting behaviour. To each of these states we have applied the following approach.

- We have computed the mutual information between each pair of subsystems corresponding to one point, as described in Section 1.3, equation (1.20). Then we have converted this information into the distances $d(A,B)$ between each pair of points

$$d(A,B) = -\ln(I(A,B)/I_{\max}). \tag{3.1}$$

  The choice of the distance function is motivated by [6] and the idea is, that for the lowest information ($I(A,B) = 0$) the distance is maximal (infinite) and for maximal information the distance is 0 (the information is maximal, when the entropy corresponding to each point is maximal, that is for maximally non-discriminating state, and the combined state of the two subsystems is in pure state, in our case $I_{\max} = 2\ln(2)$).

- We have used the acquired distances as an input for the exact embedding procedure described in Section 2.1. The results can not quite yet be interpreted as some familiar geometric structure, as the dimensionality of the resulting embedding is often similar to the number of points (while we would like a fixed dimension regardless of the number of points being embedded).

- Lastly, we have also used the MDS for computation of the embedding of the points into metric space, which is in detail described in 2.2. We have also attempted to point out some interesting features between the embeddings, if there were any.

Now follows a short description of each type of the state used together with the visualisations of its embedding. If not stated otherwise, all computations were done for a set of 20 points.

Random state I: This state is acquired by assigning a random number from inside the complex unit circle to each of the basis vectors of $\mathscr{H}_{tot}$, summing those and then normalizing the resulting vector. The problem with this state is that it takes all the small Hilbert spaces on equal footing. Thus, the resulting embedding of the points is almost always $N-1$-dimensional, which is the maximum dimension for N points. Therefore, the attached pictures serve only little illustrative purpose, as these can show only 3 dimensions at most.

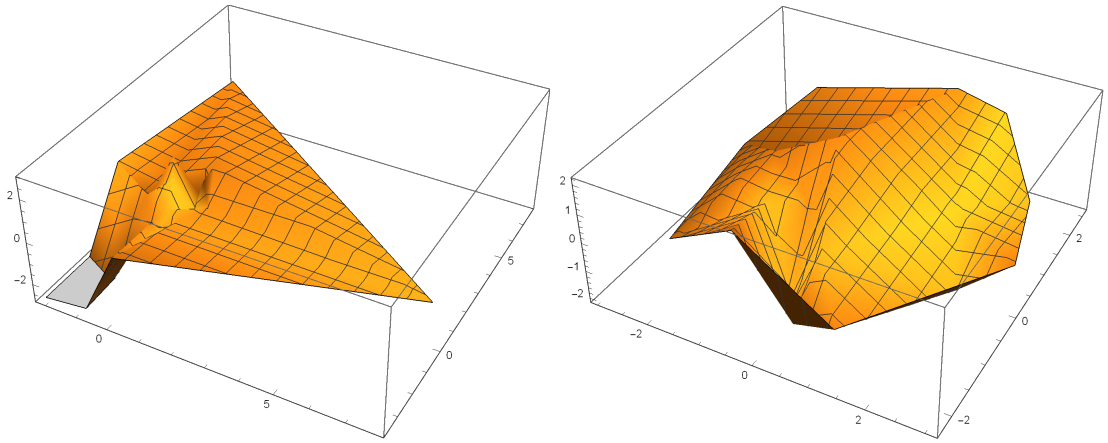

a) Exact b) MDS

Figure 3.1: Example of embedding of the Random state I.

What is to note though is that if one centres both acquired embeddings (translates them so the average distance from the origin in each of the dimensions is zero) and computes the distances from the origin, he or she than finds that the distances are the same (see Figure 3.2). Surprisingly, one does not even need to order the distances. As the embeddings also preserve the distances by definition, it is likely that one should be able to rotate one embedding onto the other.

```
Distance by exact embedding   { 8.86  8.84  8.69  9.13  8.88  8.62  8.45  8.64  8.92  8.9  9.01  8.71  8.57  9.1  8.96  8.84  8.58  8.85  9.21  8.61 }
Distance from exact embedding { 8.86  8.84  8.69  9.13  8.88  8.62  8.45  8.64  8.92  8.9  9.01  8.71  8.57  9.1  8.96  8.84  8.58  8.85  9.21  8.61 }
    Ratio of the distances    { 1.  1.  1.  1.  1.  1.  1.  1.  1.  1.  1.  1.  1.  1.  1.  1.  1.  1.  1.  1. }
```

Figure 3.2: Distances computed for Random state I for both embedding methods and comparison of the results

Random state II: In this case each of the above described basis states of $\mathscr{H}_{tot}$ were assigned a random number from the circumference of the complex unit circle and the resulting total vector was normalized. Once more, a 3D projection of the whole embedding is plotted in the Figure 3.3.

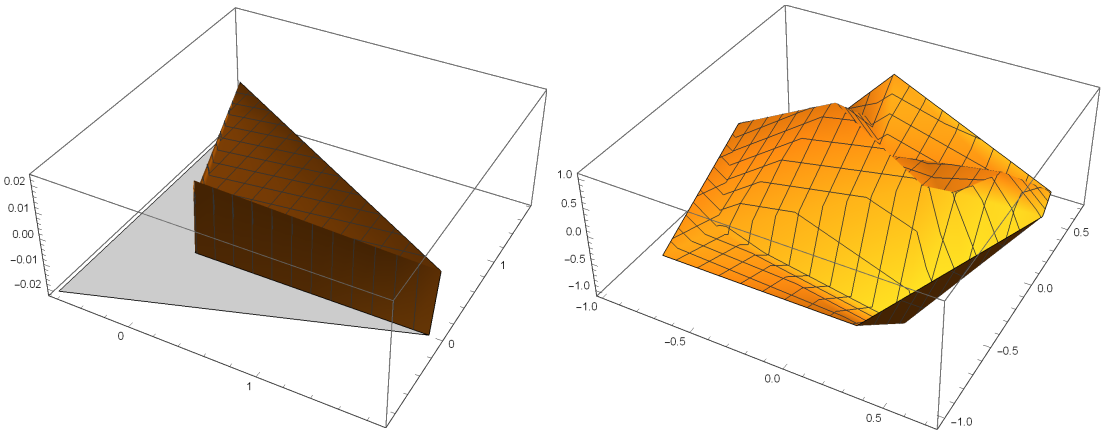

a) Exact b) MDS

Figure 3.3: Example of embedding of the Random state II.

The behaviour is very similar to that of Random state I but now the embeddings resemble even more points on $N-1$ sphere. This claim is based on the fact that the average distance of the points from the origin for Random state I grows with the number of points (e.g. for $N = 12$ the average distance is about 5 and for $N = 16$ it is about 7) but for Random state II the average distance remains in the range $\langle 2{,}3 \rangle$ for all N between 10 and 20. Also the distances from the origin are equal among the two embeddings of Random state II, the same as they were in the previous case, until $N = 16$.

Interestingly enough, for $N > 16$ the exact embedding remains 15-dimensional while the MDS retains full dimensionality. This phenomenon was realized only lately and is to be studied in the future, especially when embeddings with larger N will be available. Also there is an interesting effect that the exact embedding gives very small distances to few of the last points, otherwise the distances are fairly similar between the two approaches, as can be seen in Figure 3.4.

```
Distance by exact embedding    { 2.1  2.1  2.1  2.09  2.1  2.1  2.1  2.1  2.09  2.09  2.09  2.1  2.1  2.1  2.1  2.1  0.02  0.02  0.02  0.02 }
      Distance by MDS          { 2.11  2.11  2.11  2.11  2.11  2.11  2.11  2.11  2.11  2.11  2.11  2.11  2.11  2.11  2.11  2.11  2.11  2.11  2.11  2.11 }
  Ratio of the distances       { 0.99  0.99  0.99  0.99  0.99  0.99  0.99  0.99  0.99  0.99  0.99  0.99  0.99  0.99  0.99  0.99  0.01  0.01  0.01  0.01 }
```

Figure 3.4: Distances computed for Random state II for both embedding methods and comparison of the results

State with linear amplitude: Assuming a fixed order of the subspaces $\mathscr{H}_i$ forming $\mathscr{H}_{tot}$ each basis vector can be represented as a series of 0's and 1's. Such series can in turn be understood as a set of binary numbers. In this case each basis state was attributed with a real amplitude of the magnitude proportional to the magnitude of this binary number corresponding to the state. The total state was then normalized. Similarly to preceding cases both of the resulting embeddings are $N-1$ dimensional, so this result can also not be interpreted as some known geometry. The 3D projections to the chosen set of coordinates are shown in Figure 3.5.

It can be seen from Figures 3.6 and 3.5 that the exact embedding is highly degenerate in this case. One could expect to find traces of the linearity of the

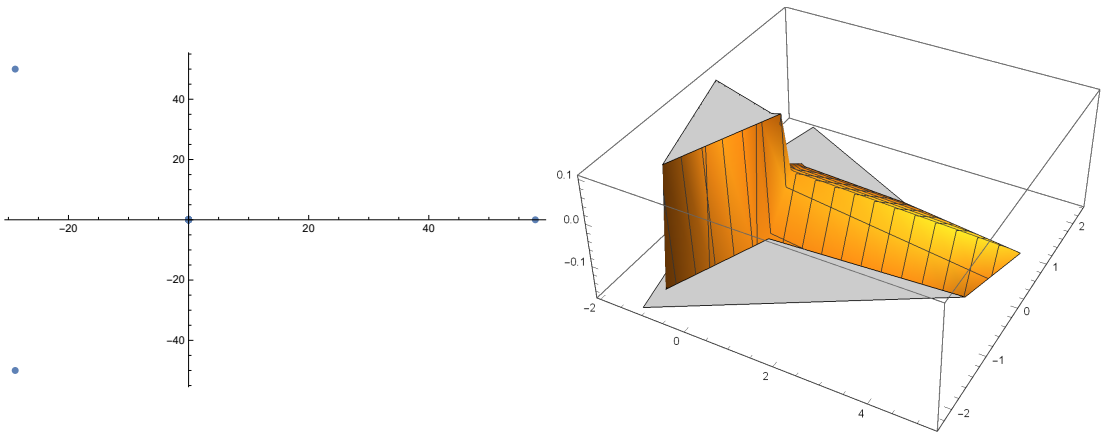

a) Exact b) MDS

Figure 3.5: Example of embedding of the State with linear amplitude. The exact embedding has degenerated to only 4 points in two dimensions.

amplitudes in the data, but we had no success in this direction. Admittedly the dependence of the distance on the initial state is complicated and so this negative result is not very surprising.

```
Distance by exact embedding                    ( 57.74 57.74 57.74 0. 0. 0. 0. 0. 0. 0. 0. 0. 0. 0. 0. 0. 0. 0. 0. 0. )
      Distance by MDS       ( 89.26 89.26 89.26 91.39 39.96 39.83 39.78 39.8 39.87 23.34 22.72 22.19 21.74 21.38 21.1 20.88 20.72 20.61 20.51 20.39 )
   Ratio of the distances                      ( 0.65 0.65 0.65 0. 0. 0. 0. 0. 0. 0. 0. 0. 0. 0. 0. 0. 0. 0. 0. 0. )
```

Figure 3.6: Values of the distances from the origin of the embedded points for State with linear amplitude. As the exact embedding is highly degenerate, this offers little informative value.

Lattice-like state I: Next state included in this text is an attempt to force a specific dimension to the embedding. Assume two integers A, B such, that $N = A \cdot B$. Now imagine a set of points positioned at the intersections of a square grid, forming there the shape of A times B rectangle. Let the points of the rectangle represent the 2-dim subspaces of the total Hilbert space. If the projection of a state onto a subspace corresponding to given point is $|0\rangle$, the point is drawn an empty circle. If the projection is $|1\rangle$, the point is a full circle. For better idea see Figure 3.7.

The aim was to choose those basis states which respect this 2-dimensional structure by attributing them with amplitude 1 in the decomposition of the state used for the computation of the information (the rest of the basis states were assigned 0). In the case of Lattice-like state I the chosen basis states were such, that for given point in the grid all the neighbouring points were in the state $|1\rangle$ and the rest of the states were $|0\rangle$ with periodic boundary condition, for better idea see Figure 3.8.

The resulting embeddings are shown in the Figure 3.9. In this case the dimensionality of the embedding is much lower, even though different for each approach. The reason is probably the following. For this state the embedding into flat space has some deviations. Both of the methods react to these deviations differently. While the exact embedding has several conditions on dimensionality, which must

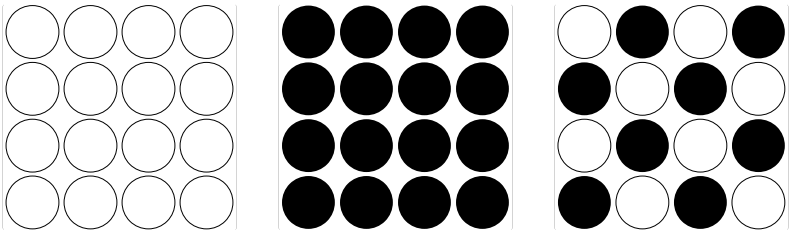

Figure 3.7: The left most schema is a grid representation of a state $|\psi_1\rangle = \bigotimes_{i=1}^{16} |0\rangle$, the middle corresponds to $|\psi_2\rangle = \bigotimes_{i=1}^{16} |1\rangle$ and the last one represents a state with alternating $|0\rangle$'s and $|1\rangle$'s

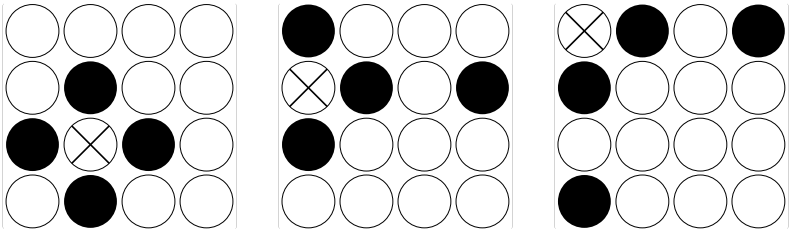

Figure 3.8: Three examples of the representations of the basis states chosen to appear in the Lattice-like state I. The crossed out point is the referential one and as in Figure 3.7 black points are attributed $|1\rangle$ and the white (including the crossed out one) are assigned $|0\rangle$

be met (volume of the n-simplices built from the embedded points must be real and non-zero, also the triangular inequality must be satisfied), the MDS can be deployed always, but some of the coordinates might be complex. In case as this we do not know how to compare the embeddings closely. So the only general result is that such specially constructed state highly reduces the final dimensionality of the embedding at the cost of problems with interpreting the output.

Lattice-like state II This case is very similar to the previous one, only now for given point such state is chosen, which has $|1\rangle$'s at the neighbouring sites and at the central site too. For clarity see Figure 3.11.

The character of the embedding is similar to that of Lattice-like state I and its 3D projection can be found in Figure 3.12.

Weighted state: This state is based on the following idea. As already mentioned above, the basis states of $\mathscr{H}_{tot}$ can be interpreted as binary numbers. So each of the basis states was assigned integer equal to the sum of 1's in the binary representation of the state. The sum of the basis states weighted in this way was then normalized. The resulting embeddings can be seen in the Figure 3.14 and the comparison of the distances given by the embeddings is in Figure 3.15.

While the embeddings themselves have similar properties as those of Random state I and II (both embeddings are $N-1$ dimensional), its surprising property is that all the embedded points have exactly the same distance from the origin and so lie on the surface of a $N-1$ sphere.

Gaussian state: In the case of this state there is at least some interesting and

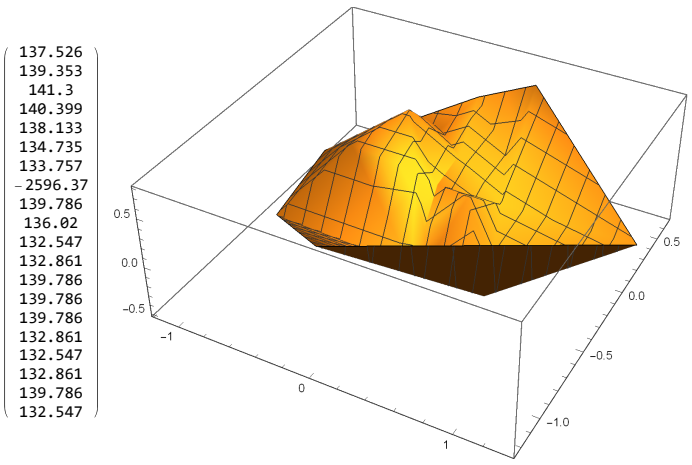

a) Exact b) MDS

Figure 3.9: Example of embedding of the Lattice-like state I. The exact embedding gave only one-dimensional result.

```
Distance by exact embedding  ( 137.53  139.35  141.3  140.4  138.13  134.73  133.76  2596.37  139.79  136.02  132.55  132.86  139.79  139.79  139.79  132.86  132.55  132.86  139.79  132.55 )
      Distance by MDS                ( 27.58  43.14  101.02  27.85  27.51  27.64  28.04  100.99  33.46  27.79  33.37  33.21  33.37  27.99  43.18  43.15  43.2  33.35  33.22  33.35 )
  Ratio of the distances                      ( 4.99  3.23  1.4  5.04  5.02  4.88  4.77  25.71  4.18  4.89  3.97  4.  4.19  4.99  3.24  3.08  3.07  3.98  4.21  3.97 )
```

Figure 3.10: Distances computed for Lattice-like state I for both embedding methods and comparison of the results

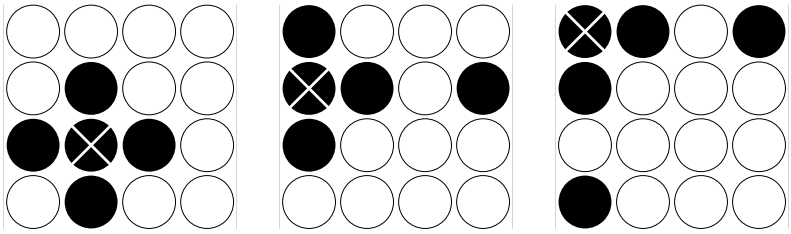

Figure 3.11: Three examples of the representations of the basis states chosen to appear in the Lattice-like state II. This time also the crossed out point is assigned $|1\rangle$, the white points remain with $|0\rangle$ in all cases

easy to discover geometrical feature. Imagine an real axis, interval of which is covered uniformly by points where each point corresponds to one basis state of $\mathscr{H}$ and from left to right the corresponding states have uniformly rising binary representation (so the left-most point corresponds to all zeros and the right-most to all ones). Now assume a Gaussian over the set of these points centred at the middle of the interval and with σ being one sixth of the length of the interval (so all points are within 3σ interval from the centre). Values of the distribution projected onto the points in the interval were then interpreted as the amplitudes for corresponding states and the state was normalized.

In the Figure 3.16 the MDS part is important. Most of the points exhibit a linear behaviour being sorted into one only slightly curved line. For this embedding also the distortion defined by (2.15) and found in Figure 3.16 in the last line is interesting, because unlike other cases here it drops quite quickly. This

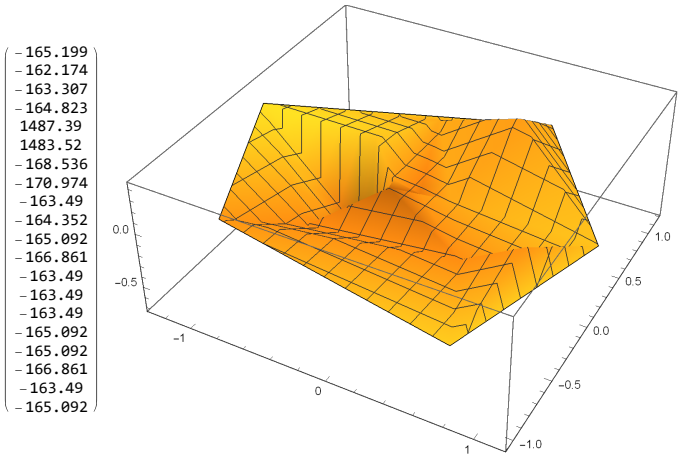

a) Exact b) MDS

Figure 3.12: Example of embedding of the Lattice-like state II.

```
Distance by exact embedding    ( 165.199  162.174  163.307  164.823  1487.39  1483.52  168.536  170.974  163.49  164.352  165.092  166.861  163.49  163.49  163.49  165.092  165.092  166.861  163.49  165.092 )
Distance from exact embedding  ( 61.3794  21.6629  21.667  73.6562  94.2461  76.7538  21.6112  67.0732  61.3267  95.8501  42.8595  21.5519  21.4607  42.8826  42.8199  46.3918  21.2426  21.3681  46.4046  57.8908 )
Ratio of the distances         ( 2.69145  7.48626  7.53715  2.23773  15.782  19.3282  7.79857  2.54907  2.66588  1.71468  3.85193  7.7423  7.61812  3.8125  3.81808  3.55864  7.77172  7.8089  3.52314  2.85178 )
```

Figure 3.13: Distances computed for Lattice-like state II for both embedding methods and comparison of the results

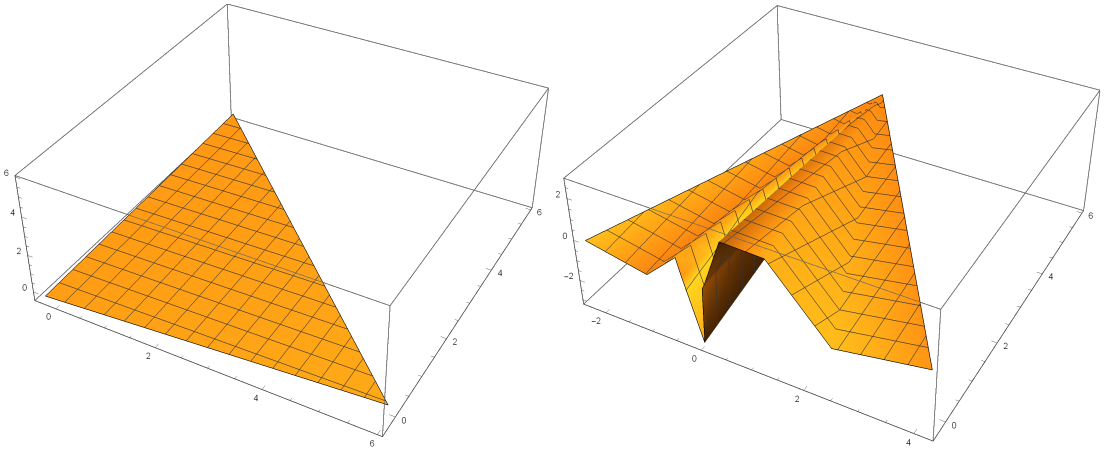

a) Exact b) MDS

Figure 3.14: Example of embedding of the Weighted state.

```
Distance by exact embedding  ( 5.95  5.95  5.95  5.95  5.95  5.95  5.95  5.95  5.95  5.95  5.95  5.95  5.95  5.95  5.95  5.95  5.95  5.95  5.95  5.95 )
      Distance by MDS        ( 5.95  5.95  5.95  5.95  5.95  5.95  5.95  5.95  5.95  5.95  5.95  5.95  5.95  5.95  5.95  5.95  5.95  5.95  5.95  5.95 )
  Ratio of the distances                    ( 1.  1.  1.  1.  1.  1.  1.  1.  1.  1.  1.  1.  1.  1.  1.  1.  1.  1.  1.  1. )
```

Figure 3.15: Distances computed for Weighted state for both embedding methods and comparison of the results

hints that some of the dimensions can be omitted and while not exactly, this

embedding is close to be of very lower dimension than $N-1$ [4]. Admittedly we seek some more complicated structures as 2 and 3D lattices, but this might be a start towards such goals.

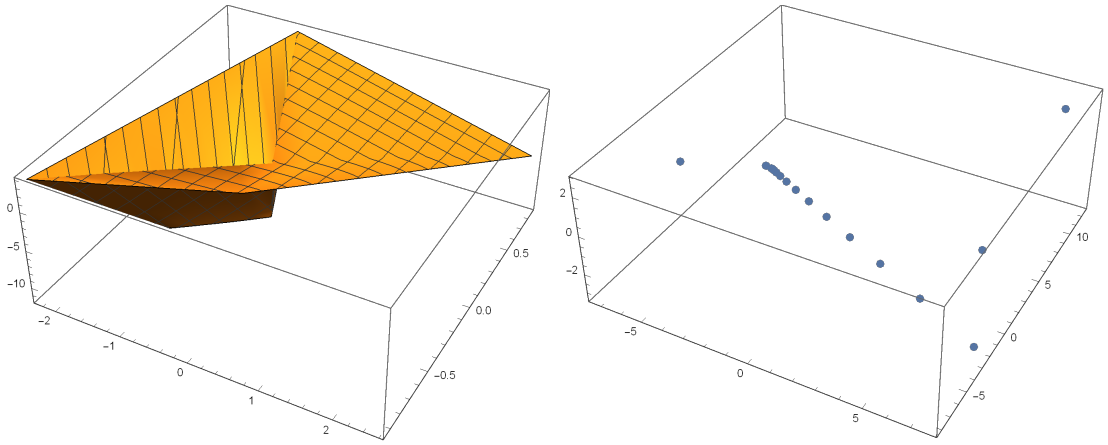

a) Exact b) MDS

Figure 3.16: Example of embedding of the Gaussian state. The MDS result was not interpolated with the mesh so the linear structure of the embedding is easily observed.

```
Distance by exact embedding   ( 26.39  20.04  17.91  16.73  15.59  13.87  12.79  11.77  10.82  9.95  9.16  8.46  7.85  7.33  6.89  6.55  6.29  6.14  6.29  6.26 )
      Distance by MDS         ( 26.39  20.04  17.91  16.73  15.59  13.87  12.79  11.77  10.82  9.95  9.16  8.46  7.85  7.33  6.89  6.55  6.29  6.14  6.29  6.26 )
   Ratio of the distances                                  ( 1.  1.  1.  1.  1.  1.  1.  1.  1.  1.  1.  1.  1.  1.  1.  1.  1.  1.  1.  1. )
Distortion parameter from MDS      {0.88, 0.8, 0.72, 0.64, 0.57, 0.51, 0.46, 0.41, 0.36, 0.31, 0.27, 0.24, 0.2, 0.17, 0.14, 0.11, 0.08, 0.06, 0.03, 0.}
```

Figure 3.17: Distances computed for Gaussian state for both embedding methods and comparison of the results

[4] For example in [6] they approved an embedding with distortion $\epsilon = 0.42$ as satisfactory in one case

4. Conclusion

It has been shown in this work, that entropy can serve as a bridge between General Relativity and Quantum Physics, the two fields current Physics seeks to connect. The fact that this problem is better understood from the quantum side leads to the assumption that GR could be derived from quantum considerations. Many modern fields of Theoretical Physics are tackling with this problem (e.g. AdS/CFT correspondence and the connected Holography principle or Loop Quantum Gravity).

Also a few commonly known features of entropy were recapitulated. Moreover some new approaches were shown, which became the core of computational part of this work (the idea of Redundancy constrained states). The computational part itself brought little results, but it has been shown that the task of finding Hilbert space with decomposition and state all together interpretable as a part of a geometry is to be expected to be a formidable task. Some experience was gained in the problems of employing the embedding methods and tracing large matrices. From the more theoretic point of view the Area Law of entropy was summarized, whose origin is in GR, but it was shown to be a result of also Quantum considerations.

This work only scratched the surface of the problem and there is yet much work to be done. In the theoretical direction there are many interesting theories that study the connection between geometry and quantum fields and which could be helpful for the advancement of the topic of this work (at least AdS/CFT needs to be mentioned here, as it sparked many of the entropic consideration in e.g. [6]). On the computational note there are many works dealing with problems of lattice of binary quantum bits thanks to the big interest in Quantum Computing. It is possible that some results acquired there might be relevant for our work. Also there are some more complex but also more powerful approaches as Tensor Networks. Or the idea of Coarse Graining (regrouping the factors of the total Hilbert space into larger groups and computing entropy between those). According to [6] this might be able to simulate the development in time.

Last but certainly not least I would like to thank my supervisor Martin Scholtz for his guidance and devotion to helping me understand this complicated topic.

Bibliography

[1] Juan Maldacena. The Large N Limit of Superconformal field theories and supergravity. *International Journal of Theoretical Physics - Springer*, 38(4):1113–1133, 1999.

[2] Horacio Cassini. Relative entropy and the Bekenstein bound. *Classical and Quantum Gravity*, 25, 2008.

[3] Leonard Susskind and James Lindesay. *An Introduction to Black Holes, Information and the String Theory Revolution: The Holographic Universe*. World Scientific Publishing Company, 1 edition, 12 2004.

[4] Roger Penrose. *Cycles of Time: An Extraordinary New View of the Universe*. The Bodley Head, 12 2010.

[5] Mark Srednicki. Entropy and Area. *Physical Review Letters*, 71(5):666–669, 1993.

[6] ChunJun Cao, Sean M. Carroll, and Spyridon Michalkis. Space from Hilbert space: Recovering geometry frum bulk entanglement. *Physical Review D*, 95(2), 2017.

[7] Ning Bao, Sean M. Carroll, and Ashmeet Singh. The Hilbert Space of Quantum Gravity Is Locally Finite-Dimensional. *International Journal of Modern Physics D*, 26(12), 2017.

[8] G. H. Hardy and S. Ramanujan. The normal number of prime factors of a number n. *Quaterly Journal of Mathematics*, 48:76–92, 1917.

[9] Jason Pollack and Ashmeet Singh. Towards space from Hilbert space: finding lattice structure in finite-dimensional quantum systems. *Quantum Studies: Mathematics and Foundations*, pages 1–20, 2018.

[10] E M Lifshitz and I M Khalatnikov. Investigations in relativistic cosmology. *Advances in Physics*, 12(46):185–249, 1963.

[11] Roger Penrose. Gravitational Collapse and Space-Time Singularities. *Physical Review Letters*, 14(3):57–59, 1965.

[12] B Carter. Axisymmetric Black Hole Has Only Two Degrees of Freedom. *Physical Review Letters*, 26(6):331–333, 1971.

[13] S W Hawking and G F R Ellis. The large scale structure of space-time, 1973.

[14] D C Robinson. Uniqueness of the Kerr Black Hole. *Physical Review Letters*, 34(14):905–906, apr 1975.

[15] Yong-Qiang Wang, Yu-Xiao Liu, and Shao-Wen Wei. Excited Kerr black holes with scalar hair. *Physical Review D*, 99(6):64036, 2018.

[16] J M Bardeen, B Carter, and S W Hawking. The four laws of black hole mechanics. *Communications in Mathematical Physics*, 31(2):161–170, 1973.

[17] R M Wald. Entropy and black-hole thermodynamics. *Physical Review D*, 20:1271–1282, sep 1979.

[18] R M Wald. *General Relativity*. The University of Chicago Press, 1984.

[19] S W Hawking. Gravitational Radiation from Colliding Black Holes. *Phys. Rev. Lett.*, 26(21):1344–1346, may 1971.

[20] Norman Gürlebeck and Martin Scholtz. Meissner effect for weakly isolated horizons. *Physical Review D*, 95(6), 2017.

[21] Norman Gürlebeck and Martin Scholtz. Meissner effect for axially symmetric charged black holes. *Physical Review D*, 97(8):084042, apr 2018.

[22] J Lewandowski and T Pawlowski. Extremal isolated horizons: a local uniqueness theorem. *Classical and Quantum Gravity*, 20(4):587–606, 2003.

[23] R Penrose. The question of cosmic censorship. *Journal of Astrophysics and Astronomy*, 20(3):233–248, dec 1999.

[24] Jakob D. Bekenstein. Black holes and entropy. *Physical Review D*, 7(8):2333–2346, 1973.

[25] Stephen William Hawking. Particle creation by black holes. *Communications in Mathematical Physics*, 43(2):199–220, 1975.

[26] L Parker. Particle Creation in Expanding Universes. *Phys. Rev. Lett.*, 21(8):562–564, aug 1968.

[27] N D Birrel and P C W Davies. *Quantum fields in curved space*. 1982.

[28] W G Unruh. Origin of the particles in black-hole evaporation. *Physical Review D*, 15:365–369, jan 1977.

[29] Maulik K. Parikh and Frank Wilczek. Hawking radiation as tunnelling. *Physical Review Letters*, 85:5042–5045, 2000.

[30] J B Hartle and S W Hawking. Path-integral derivation of black-hole radiance. *Phys. Rev. D*, 13(8):2188–2203, apr 1976.

[31] G W Gibbons and S W Hawking. Action integrals and partition functions in quantum gravity. *Phys. Rev. D*, 15(10):2752–2756, may 1977.

[32] Adam D Helfer. Do black holes radiate? *Reports on Progress in Physics*, 66(6):943–1008, 2003.

[33] S W Hawking. Breakdown of predictability in gravitational collapse. *Physical Review D*, 14(10):2460–2473, nov 1976.

[34] R Penrose. Republication of: Conformal treatment of infinity. *General Relativity and Gravitation*, 43(3):901–922, 2011.

[35] J Stewart. *Advanced General Relativity*, volume -1. 1993.

[36] R Penrose. *Techniques of Differential Topology in Relativity.* CBMS-NSF Regional Conference Series in Applied Mathematics. Society for Industrial and Applied Mathematics, 1972.

[37] L Susskind, L Thorlacius, and J Uglum. The stretched horizon and black hole complementarity. *Phys. Rev. D*, 48(8):3743–3761, oct 1993.

[38] Beth A. Brown and James Lindesay. Construction of a Penrose diagram for a spatially coherent evaporating black hole. *Classical and Quantum Gravity*, 25(10), 2008.

[39] W K Wootters and W H Zurek. A single quantum cannot be cloned. *Nature*, 299(5886):802–803, 1982.

[40] Jakob D. Bekenstein. Universal upper bound on the entropy-to-energy ratio for bounded systems. *Physical Review D*, 23(2):287–298, 1981.

[41] Raphael Bousso, Horacio Cassini, Zachary Fisher, and Juan Maldacena. Proof of a quantum Bousso bound. *Physical Review D*, 90, 2014.

[42] Don N. Page. Information in Black Hole Radiation. *Physical Review Letters*, 71(23):3743–3746, 1993.

[43] D Page. Average enropy of a subsystem. *Physical review letters*, 71(August):1291–1294, aug 1993.

[44] S. K. Foong and S. Kanno. Proof of page's conjecture on the average entropy of a subsystem. *Phys. Rev. Lett.*, 72:1148–1151, Feb 1994.

[45] Giovanni Acquaviva, Alfredo Iorio, and Martin Scholtz. On the implication of the Bekenstein bound for black hole evaporation. *Annals of Physics*, 387:317–333, 2017.

[46] Alfredo Iorio. Weyl-gauge symmetry of graphene. *Annals of Physics*, 326(5):1334–1353, 2011.

[47] A Iorio, G Lambiase, and G Vitiello. Entangled quantum fields near the event horizon and entropy. *Annals of Physics*, 309(1):151–165, 2004.

[48] Alfredo Iorio and Gaetano Lambiase. Quantum field theory in curved graphene spacetimes, Lobachevsky geometry, Weyl symmetry, Hawking effect, and all that. *Physical Review D - Particles, Fields, Gravitation and Cosmology*, 90(2):1–28, 2014.

[49] A Fabbri and J Navarro-Salas. *Modeling Black Hole Evaporation.* Imperial College Press, 2005.

[50] C.L. Morgan. Embedding metric spaces in Euclidean space. *Journal of Geometry*, 5(1):101–107, 1974.

[51] James E. Gentle. *Statistics and Computing: Numerical Linear Algebras for Applications in Statistics.* Springer Science+Business Media, 1nd edition, 1998.

[52] Ingwer Borg and Patrick J.F. Groenen. *Modern Multidimensional Scaling - Theory and Applications*. Springer Science+Business Media, 2nd edition, 2005.

A. Mathematica code

In the appendix the code from Mathematica 11.3.0.0 used to acquire the results shown in this work is summarized. It is divided into cells as is usual for Mathematica Notebook. While the layout of the code might not be visually ideal, it was created in order not to divide commands among multiple pages.

A.1: Initialization cell

```
In[*]:= (*Number of points used in the computation. Use max 16 for trial purposes and max 22 for the
 computation not to last more than 1 day on average PC.*)
varNOfPoints = 12;

(*The following option is needed for experimental states 7 and 8,
the product of the numbers should be equal to varNOfPoints*)
varLatticeDimensions = {3, 4};

(*Important note: varDimensions fields correspond to the subsystems from left to right (because also )*)
varDimensions = Table[2, {i, varNOfPoints}];

(*Check, if length of the list Dimensions is equal to the number of points.*)
"Number of dimensions is equal to the number of points: " <> ToString[varNOfPoints == Length[varDimensions]]

(*Check, if the dimensions are integer*)
"Dimensions are integer: " <> ToString[ArrayQ[varDimensions, _, IntegerQ]]

(*Number of basis states, characterizes well the overall complexity of the computation*)
varComplexity = Times @@ varDimensions;

(*Converts integer representing an ordinal number of a basis vector to that basis vector*)
funcIntegerToList[i_Integer] := Module[{locvarInt = i, locvarOutput = {}, j = 1},
   While[
    j ≤ varNOfPoints,
    PrependTo[locvarOutput, Mod[locvarInt, varDimensions[[-j]]]];
    locvarInt = Quotient[locvarInt, varDimensions[[-j]]];
    j++
   ];
   locvarOutput
  ];

(*Generates all basis vectors*)
varBasis = funcIntegerToList[#] & /@ (Range[0, varComplexity - 1]);

(*Converts a basis vector to its ordinal number*)
funcListToInteger[l_List] := Total[Table[l [[-k]] (varDimensions[[-k]]^(k - 1)), {k, 1, Length[l]}]];
```

```
(*The following function computes the reduced matrix based on the full density matrix
 corresponding to the state 'varState'. It computes the trace over all of the basis subsystems
 but those specified by the integers in the input list 'points'*)

funcReduceMatrixFromState[points_List, state_List] :=
  Module[{locvarOrderedList = Sort[points, Greater], locvarStartIterators = {}, locvarIterators = {},
    locvarIndexOfTraced = Complement[Range[varNOfPoints], points], locvarStart, locvarStartJumps,
    locvarVectorJumps, locvarVector, locvarOutput},

   If[locvarIndexOfTraced == {}, Outer[Times, state, Conjugate[state]],

    locvarStartIterators = Table[{j[i], 0, varDimensions[[i]] - 1}, {i, locvarIndexOfTraced}];

    locvarStartJumps = Total@((j[#] Times @@ varDimensions[[1 ;; # - 1]]) & /@ locvarIndexOfTraced);

    locvarStart = Flatten[Table[locvarStartJumps, Evaluate[Sequence @@ locvarStartIterators]]];

    locvarIterators = Table[{j[i], 0, varDimensions[[i]] - 1}, {i, points}];

    locvarVectorJumps = Total@((j[#] Times @@ varDimensions[[1 ;; # - 1]]) & /@ points);

    locvarVector = Flatten[Table[# + locvarVectorJumps, Evaluate[Sequence @@ locvarIterators]]] & /@
      locvarStart;

    locvarOutput = Total[Outer[Times, #, Conjugate[#]] & /@ (state[[#]] & /@ (locvarVector + 1))];

    locvarOutput
   ]
  ];

(*Computes the distance based on information. There is a hard set maximal distance,
in order to avoid infinites in the cases of degenerate results. Such results are not interesting
 in any case, but in this way one avoid clutter with infinites and indeterminate expressions*)
funcDistanceFunction[info_, order_] :=
 If[Chop[info[[order, 1]]] == 0, 30, Chop[-Log[info[[order, 1]]] / (2 Log[2])]]]
```

A.2: Cell for determination of the type of state for further work and computation of the distances between the points represented by this state

```
(*Measurment of the time the computation of the reduced matrices starts here
 (there are some commands before the actual tracing starts,
   but these take little time to influence the result).*)
varTime = AbsoluteTime[];

(*Library of states*)

(*(1) - State with fully random amplitude and phase for each basis vector.*)
varStateAllRandom = Normalize[Table[(#1 Exp[2 Pi I #2]) &@@ RandomReal[{0, 1}, 2], {i, varComplexity}]];

(*(2) - State with uniform amplitude and random phase*)
varStateRandomPhase = Normalize[Table[Exp[2 Pi I #] &@@ RandomReal[{0, 1}], {i, varComplexity}]];

(*(3) - State with linearly rising amplitude and constant phase*)
varStateLinearAmp = Normalize[Table[i, {i, varComplexity}]];

(*(4)- State with gaussian distribution of amplitudes and constant phase*)
varStateGaussian =
  Normalize[Table[N[PDF[NormalDistribution[Quotient[varComplexity, 2], Quotient[varComplexity, 6]]][i]],
    {i, varComplexity}]];

(*Excluded (5)- State with constant amplitudes but opposite phases between each two neighbours.
   Reason for excluding - gives zero entropy*)
varStateOppositePhase = Normalize[Table[(-1)^i, {i, varComplexity}]];

(*Excluded (6)- State with constant phase and amplitude
  Reason for excluding - gives zero entropy*)
varStateConstant = Normalize[Table[1, {i, varComplexity}]];
```

```
(*(7) - Attempting to find a state for lattice-
 like positioning of the points with binary Hilbert space at each point.*)
varLatticeBasis = Module[{locvarInstructions},

   (*This contains the instructions, which "spins" to flip for each vector creating the total
    vector used for further computation*)
   locvarInstructions = Flatten[Table[

      varTMP1 = i + varLatticeDimensions[[1]] j;

      {1 + varTMP1 → 1, (*choosen point*)
       1 + varLatticeDimensions[[1]] j + Mod[varTMP1 + 1, varLatticeDimensions[[1]]] → 1,
       (*the point to the right*)
       1 + varLatticeDimensions[[1]] j + Mod[varTMP1 - 1, varLatticeDimensions[[1]]] → 1,
       (*the point to the left*)
       1 + (j - Mod[j, varLatticeDimensions[[2]]] + Mod[j + 1, varLatticeDimensions[[2]]])
          varLatticeDimensions[[1]] + i → 1, (*the point above*)
       1 + (j - Mod[j, varLatticeDimensions[[2]]] + Mod[j - 1, varLatticeDimensions[[2]]])
          varLatticeDimensions[[1]] + i → 1(*the point below*)},

      {i, 0, varLatticeDimensions[[1]] - 1}, {j, 0, varLatticeDimensions[[2]] - 1}]

     , 1];

   Reverse[ReplacePart[Table[0, {i, Times @@ varLatticeDimensions}], #]] & /@ locvarInstructions

  ];



varExperimentalState1 =
  Normalize[ReplacePart[Table[0, {i, varComplexity}], # → 1 & /@ (funcListToInteger /@ varLatticeBasis)]];

(*(8) - Attempting to find a state for lattice-
 like positioning of the points. (Alternate approach - the central point is omitted)*)
varLatticeBasis = Reverse[ReplacePart[Table[0, {i, Times @@ varLatticeDimensions}], #]] & /@ Flatten[Table[

     varTMP1 = i + varLatticeDimensions[[1]] j;

     {1 + varLatticeDimensions[[1]] j + Mod[varTMP1 + 1, varLatticeDimensions[[1]]] → 1,
      (*the point to the right*)
      1 + varLatticeDimensions[[1]] j + Mod[varTMP1 - 1, varLatticeDimensions[[1]]] → 1,
      (*the point to the left*)
      1 + (j - Mod[j, varLatticeDimensions[[2]]] + Mod[j + 1, varLatticeDimensions[[2]]])
         varLatticeDimensions[[1]] + i → 1, (*the point above*)
      1 + (j - Mod[j, varLatticeDimensions[[2]]] + Mod[j - 1, varLatticeDimensions[[2]]])
         varLatticeDimensions[[1]] + i → 1(*the point below*)},

     {i, 0, varLatticeDimensions[[1]] - 1}, {j, 0, varLatticeDimensions[[2]] - 1}],

    1];


varExperimentalState2 =
  Normalize[ReplacePart[Table[0, {i, varComplexity}], # → 1 & /@ (funcListToInteger /@ varLatticeBasis)]];
```

```
(*(9) -
 Weighted state: Each basis vector is given the weight corresponding to the number of 1's in
    its binary representation.*)
varWeightedState = Normalize[Table[Total[varBasis[[i]]], {i, Length[varBasis]}]];

(*(10) -
 Modified weighted
  state: Chosen basis vectors are attributed weight corresponding to their binary representation.*)
varWeightedState2 = Table[0, {i, varComplexity}];
(varWeightedState2[[# + 1]] = 1 / #) & /@
  Table[funcListToInteger@Table[If[j ≥ i, 1, 0], {j, varNOfPoints}], {i, varNOfPoints}];
varWeightedState2 = Normalize[varWeightedState2];

(*(11) - Modified weighted state with random
  phase: Chosen basis vectors are attributed weight corresponding to their binary representation
    and random phase.*)
varWeightedState3 = Table[0, {i, varComplexity}];
(varWeightedState3[[# + 1]] = (1 / # ) Exp[I RandomReal[{0, 2 Pi}]]) & /@
  Table[funcListToInteger@Table[If[j ≥ i, 1, 0], {j, varNOfPoints}], {i, varNOfPoints}];
varWeightedState3 = Normalize[varWeightedState3];

(*In the following variable all the states are stored in denoted order,
so the state actually chosen for the computation can be easily reffered to in the following.*)
varStateLibrary = {varStateAllRandom, varStateRandomPhase, varStateLinearAmp, varStateGaussian,
   varStateOppositePhase, varStateConstant, varExperimentalState1, varExperimentalState2,
   varWeightedState, varWeightedState2, varWeightedState3};

varChosenState = 1;


(*Choosing the state for the following computation*)
varState = varStateLibrary[[varChosenState]];

(*The two following calls compute the entropy of a single point and between two points. For
  each computation the result is a two-field array,
first field containing the result itself and the other indices of the subsystems the entropy
 corresponds to.*)
varPairwiseEntropy =
  Chop[
   {Total[N[-Log[#] #] & /@ DeleteCases[Eigenvalues[funcReduceMatrixFromState[#, varState]], N[0] | 0]],
      #} & /@ Subsets[Range[varNOfPoints], {2}]];
varPointwiseEntropy =
  Chop[
   {Total[N[-Log[#] #] & /@ DeleteCases[Eigenvalues[funcReduceMatrixFromState[#, varState]], N[0] | 0]],
      #} & /@ Subsets[Range[varNOfPoints], {1}]];
```

```
(*The following function computes the pairwise information for all pairs while preserving
 also the information of which pair does the result correspond to.*)
funcComputeInformation[pairwise_List, pointwise_List] := Module[{locvarOutput = {}},
   For[k = 1, k ≤ Length[pairwise], k++,
    AppendTo[locvarOutput, {-pairwise[[k, 1]] + pointwise[[pairwise[[k, 2, 1]], 1]] +
        pointwise[[pairwise[[k, 2, 2]], 1]], pairwise[[k, 2]]}];
   ];
   locvarOutput
  ];

varInformationOfPairs = funcComputeInformation[varPairwiseEntropy, varPointwiseEntropy];

(*This command prepeares the table of the distances to be filled in in the next step.*)
varDistances = Table[0, {i, varNOfPoints}, {j, varNOfPoints}];

(*This fills in the table of varDistances symmetrically. Currently the formula is distance=
 -Ln[mutual information].*)
For[k = 1, k <= Length[varInformationOfPairs], k++,
  varDistances[[varInformationOfPairs[[k, 2, 1]], varInformationOfPairs[[k, 2, 2]]]] =
    varDistances[[varInformationOfPairs[[k, 2, 2]], varInformationOfPairs[[k, 2, 1]]]] =
     funcDistanceFunction[varInformationOfPairs, k];
 ];

varDistances // MatrixForm;

"The calculation took " <> ToString[AbsoluteTime[] - varTime] <> " seconds"
```

A.3: Cell that assesses the maximal dimension of the exact embedding

```
(*Choose, which point will be the origin (can be either set or randomly chosen). The number
 identifies the point by its column/row in the table of distances.
  Choosing the point in such a way can lead to translation of the final set of points after the computation,
but should not affect the result otherwise.*)
varOriginIndex = 1;

(*Definition of the triple product function accoring to the article.*)
funcTP[dist_, i_Integer, j_Integer, k_Integer] := 1 / 2 (dist[[i, k]]^2 + dist[[j, k]]^2 - dist[[i, j]]^2);

(*A boole to check later, if the dimension of the space into which the embedding will be done,
will have been computed during the calculation or will be preset*)
varMaxDimComputed = True;

(*Determination of volumes of all simplices up to the order of the number of the vertices. From the end:
  The last Range creates the set of all available orders of the simplices.
     Then the Subsets command takes appropriate n-tuples of vertices while making sure to not pick origin,
or otherwise the volume would need to be 0.
  The the main function produces the Table of triple products between all pairs from given n-
 tuple and the origin and appropriate Determinant, square Root and Normalization is done
 The results are rounded (Chopped) for very small values, for the next steps to be sensible.*)
varNOfSamplePoints = varNOfPoints - 1;
"Number of sample points ≤ total number of points: " <> ToString[varNOfSamplePoints ≤ varNOfPoints]

(*Sample points indices*)
varSamplePoints = RandomSample[DeleteCases[Range[varNOfPoints], varOriginIndex], varNOfSamplePoints];

(*Simplices volumes*)
varSimplexVolume =
  Chop[
   (1 / #1! (Sqrt[Det[Table[funcTP[varDistances, i, j, varOriginIndex], {i, #1}, {j, #1}]]] & /@
         Subsets[varSamplePoints, {#1}]) & /@ Range[varNOfSamplePoints]), 10^-7];
```

A.4: Cell that checks the triangle inequality satisfaction and computes the coordinates of the embedding

```
varCounter = 0;

"Points not satisfying the triangle inequality (if any):"
varNote = Table[
   If[varDistances[[i, j]] + varDistances[[j, k]] ≥ varDistances[[i, k]], True, Print[{i, j, k, varCounter}];
    varCounter++; False],
   {i, varNOfPoints}, {j, varNOfPoints}, {k, varNOfPoints}];

(*Check if triangle inequality is satisfied.*)
boolTriangleInequality = And @@ Flatten[varNote];
"Triangle equality is satisfied: " <> ToString[boolTriangleInequality]

(*Check if all volumes are real.*)
boolZeroImaginaryPart = Map[Im[#1] == 0 &, varSimplexVolume, {2}];
boolFlatGraph = And @@@ boolZeroImaginaryPart;
varHighestFlatDimension = Module[{locvarOutput = 0},
   While[ locvarOutput < Length[boolFlatGraph],
    If[boolFlatGraph[[locvarOutput + 1]] == True, locvarOutput++, Break[]] ;
   ];
   locvarOutput
  ];

"The highest flat dimension of the graph is: " <> ToString[varHighestFlatDimension]

(*Determination of the highest order of simplices for which there exists at least one with
 nonzero volume. It creates a List and into each field it puts either the ordinal number of the field,
if there exists a simplex of nonzero volume for given order, or 0,
if all simplices of given order have 0 volume. Then it takes the maximum as the dimension of the space,
into which the points are to be embedded. It also writes this dimension in the end.*)
varNonzeroSimplices = Table[If[varSimplexVolume[[i]] ≠ Array[0 &, Length[varSimplexVolume[[i]]]], i, 0],
   {i, varNOfSamplePoints}];
varMaxDim = Module[{locvarOutput = {}, k = 0},
   While[varNonzeroSimplices[[k + 1]] ≠ 0 && boolFlatGraph[[k + 1]],
    k++;
   ];
   k
  ];
varMaxDimComputed = True;

(*For reason of caluclational difficulty the acquisition of the dimension from the simplices
 volume can be skipped, but then the dimension of the space into which we want to embedd the
 points needs to be specified manually*)
varPresetDim = False;
varMaxDim = If[varMaxDimComputed, varMaxDim, varPresetDim];

"Maximal dimension is " <> ToString[varMaxDim]
```

```
(*The basis simplex is chosen to be the one,
whose points are in distance table specified by rows/columns {1,2,3,...} with possibly skipping the origin,
if needed.
   The function then assings to each point its coordinates in n-
 dimensional space within the basis given by the above chosen simplex.*)
varBasisSimplex = DeleteCases[Range[varNOfPoints], varOriginIndex][[1 ;; varMaxDim]];

funcF[x_Integer] := Table[funcTP[varDistances, x, varBasisSimplex[[i]], varOriginIndex], {i, varMaxDim}];
varCoordinates1 = Table[funcF[i], {i, varNOfPoints}]^T;

(*Turning the coordinates back to the cartesian coordinates
1st step: the metric of the current space is g=<x_i,x_j,x_0>^-1, i,
j goes through the vertices of the reference simplex.*)

varTableOfTP = varCoordinates1^T[[varBasisSimplex]];

(*step 2: finding the transformation matrix to cartesian space
  (basically, (u,v)=u.g.v, where u,v are vectors with coordinates with respect to the basis
    simplex' edges. What we do is, that we find R such,
   that g=RR^T and so (u,v)=u.R.R^T.v and so R^T.u and R^T.v are coordinates of u and v with respect
      to cartesian unit basis. This is called the Cholesky Decomposition*)
varTransformationMatrix = CholeskyDecomposition[(# + Transpose[#]) / 2 &@Inverse[varTableOfTP]];

(*step 3: applying the transformation to acquire the coordinates of the points in euclidean
  space with unit metric. The transpose is there in order to have the coordinates in rows
  for easier computation.*)
varCoordinates2 = (varTransformationMatrix.varCoordinates1)^T;

(*Move the points to the center, so that the average of each of their coordinates is 0*)

varCoordinatesTranslation = Table[-Total[varCoordinates2[[All, i]]] / varNOfPoints, {i, varMaxDim}];
varCoordinates2 = Map[# + varCoordinatesTranslation &, varCoordinates2, 1];

varGraphOfEmbedding3D =
 If[varMaxDim == 3, ListPointPlot3D[varCoordinates2, AspectRatio → 1, ImageSize → Large]]
varGraphOfEmbedding2D = If[varMaxDim == 2, ListPlot[varCoordinates2, AspectRatio → 1, ImageSize → Large]]
```

A.5: Computation of MDS embedding

```
(*Implementation of the multidimensional scaling*)
varB =
  Table[
   -1 / 2 (varDistances[[i, j]]^2 - Total[#^2 & /@ varDistances[[i]]] / varNOfPoints -
      Total[#^2 & /@ varDistances[[All, j]]] / varNOfPoints +
      Sum[varDistances[[k, l]]^2, {k, varNOfPoints}, {l, varNOfPoints}] / varNOfPoints^2),
   {i, varNOfPoints}, {j, varNOfPoints}];

varESystem = Eigensystem[varB];
(*Note: in transpose form the Eigensystem produces a list of pairs,
1st member of the pair being an eigenvalue and 2nd the corresponding eigenvector. So the zero
 eigenvalue and their eigenvectors can be easily deleted.*)
varESystem = DeleteCases[Chop[varESystem^T], {0, _}]^T;

varCoordinatesFromMDS =
  Table[Sqrt[varESystem[[1, i]]] Normalize[varESystem[[2, i]]], {i, Length[varESystem[[1]]]}]^T;
```

A.6: Cell that prints the resulting coordinates and checks, if both embeddings are properly centred

```
(*Comparison of results of the coordinates. Each ROW! corresponds to the coordinates of a point.*)
Chop[varCoordinates2] // MatrixForm
Chop[varCoordinatesFromMDS] // MatrixForm

(*The two following lines show that the embeddings are centered at origin*)
Table[Chop[Total[varCoordinates2[[All, i]]]], {i, Length[varCoordinates2[[1]]]}]
Table[Chop[Total[varCoordinatesFromMDS[[All, i]]]], {i, Length[varCoordinatesFromMDS[[1]]]}]
```

A.7: Cell that computes and compares the distances of individual points from the origin for both embeddings. Also computes distortion for MDS

```
(*Computing the distances from origin for all available embedding methods.*)
varDistancesFromOrigin1 = Chop[Total[#^2 & /@ varCoordinates2, {2}]]
varDistancesFromOrigin2 = Chop[Total[#^2 & /@ varCoordinatesFromMDS, {2}]]

(*Comparison of distances of the points from the origin for different embeddings.*)
varComparisonOfDistances = Table[varDistancesFromOrigin1[[i]] / varDistancesFromOrigin2[[i]],
  {i, Length[varCoordinatesFromMDS[[1]]]}]

(*Computing the distorsion. If n-th number from left is sufficiently small,
n is the number of dimensions of the space, into which the points are well embedded*)
varDistortionParameter = Table[1 - Total[varESystem[[1, 1 ;; i]]] / Total[varESystem[[1]]],
  {i, Length[varESystem[[1]]]}]
```